NSF/CEE-82122

PB84-220599

FIELD INDEX TEST FOR ESTIMATING LIQUEFACTION POTENTIAL

March 31, 1982

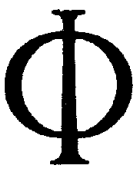

GEOTECHNICAL ENGINEERS INC.

50272-101

REPORT DOCUMENTATION PAGE	1. REPORT NO. NSF/CEE-82122	2.	3. Recipient's Accession No. PB82 220599

4. Title and Subtitle
Field Index Text for Estimating Liquefaction Potential

5. Report Date
March 1982

6.

7. Author(s)
G. Castro, D.R. Shields, J.W. France

8. Performing Organization Rept. No.

9. Performing Organization Name and Address
Geotechnical Engineers, Inc.
1017 Main Street
Winchester, MA 01890

10. Project/Task/Work Unit No.

11. Contract(C) or Grant(G) No.
(C)
(G) CEE8114111

12. Sponsoring Organization Name and Address
Division of Industrial Science and Technological Innovation (ISTI)
Directorate for Scientific, Technological, and International Affairs (STIA)
National Science Foundation, Washington, DC 20550

13. Type of Report & Period Covered
SBIR - Phase I

14.

15. Supplementary Notes

16. Abstract (Limit: 200 words)

The feasibility of using a vane shear device as an in situ index test for evaluating the susceptibility of sands to earthquake-induced liquefaction was investigated. The behavior of sands placed at known densities in a laboratory test cell equipped with a prototype vane shear was examined as the sands were subjected to drained and undrained shear loading. Tests were performed on two uniform fine sands. It was found that the drained vane shear test can be used to evaluate the liquefaction potential of sands based on the effective stress changes that occur during the test due to volume changes in the shear zone. It was concluded that an undrained shear test is not practical in clean sands because of the rapid dissipation of the shear-induced pore pressures.

17. Document Analysis a. Descriptors

Earthquakes
Liquefaction
Soils
Sands
Behavior
Tests
Stresses
Shear stress
Vane shear tests
Pressure

b. Identifiers/Open-Ended Terms

G. Castro, /PI

c. COSATI Field/Group

18. Availability Statement	19. Security Class (This Report)	21. No. of Pages
NTIS	20. Security Class (This Page)	22. Price

64

(See ANSI-Z39.18) See Instructions on Reverse

OPTIONAL FORM 272 (4-77)
(Formerly NTIS-35)
Department of Commerce

This material is based upon work supported by the National Science Foundation under Award No. CEE-8114111. Any opinions, findings, and conclusions or recommendations expressed in this publication are those of the authors and do not necessarily reflect the views of the National Science Foundation.

TABLE OF CONTENTS

LIST OF FIGURES

LIST OF FIGURES

1. INTRODUCTION

1.1 Statement of the Problem

Currently, there are two basic approaches for evaluating the susceptibility of saturated sand deposits to earthquake-induced liquefaction, namely: 1) analytical procedures based on the results of laboratory tests on high quality "undisturbed" samples and 2) an empirical approach based on correlations between the standard penetration test (SPT) blowcounts and the observed occurrence or nonoccurrence of ground failure at sites subjected to past earthquakes.

"Undisturbed" sand samples undergo unavoidable changes in density and structure during sampling and subsequent laboratory testing. Elaborate and expensive techniques for sampling and handling have been employed to minimize this disturbance, but even with the best available techniques, the error introduced by sample disturbance is not negligible and corrections must be applied to the laboratory test data. Thus, analytical procedures based on the results of laboratory tests on "undisturbed" samples are both expensive and involve significant uncertainties.

The existing empirical correlations relating the standard penetration resistance of sands, the cyclic shear stresses induced by earthquakes, and the occurrence or nonoccurrence of ground failure show a pattern separating failure and nonfailure cases, as shown in Fig. 1-1, indicating the empirical approach has promise as a reliable and economical tool in practice. There are serious limitations on both the quantity and quality of the data on which the existing correlations are based and the reliability of the standard penetration test itself. These are:

1) There is a significant range of data for which the empirical correlations indicate both failure and nonfailure conditions for the same blowcounts and earthquake shear stresses.

2) For about two thirds of the cases presented in the correlations, the ground surface acceleration, a key parameter, was not measured but was estimated from published magnitude-distance-acceleration correlations which have a great deal of scatter.

3) The data are particularly scarce in the range of strong earthquakes and relatively high blowcounts.

4) The standard penetration test data (N-values) for a given case can fluctuate over rather wide ranges within a soil deposit, and the proper selection of a representative value of N requires complete knowledge of the stratigraphy at the site. For some cases, only a brief description of the sand and a few blowcounts are available, and they may not be representative of the most critical soil layer.

5) The N-value is notoriously sensitive to the techniques used in its determination. Differences in N of as much as 50% can be obtained among reputable drillers in any given sand deposit attributable to what would appear to be only slight differences in procedure. The existing correlations are based on blowcounts obtained at sites located in several countries and obtained under unknown degrees of control and adherence to the standard procedures.

6) Factors such as stratification, water level, and soil type may affect the correlations, and their potential influence has not been satisfactorily evaluated.

The existing empirical correlations have been based on the standard penetration test because it was the most readily available index for the sites for which there was information on the actual behavior of sands during earthquakes. Other in situ tests which exhibit greater sensitivity to soil density and better repeatability than the standard penetration test may be better suited for empirical liquefaction correlations.

It is apparent from the above discussion that there exists a need for: 1) improvement of the existing empirical correlations for susceptibility to earthquake-induced liquefaction and 2) an in situ test which is better suited for such correlations than the standard penetration test on which the existing correlations are based.

1.2 Objectives of the Research Program

The major objectives of the research program are to:

1) Develop a new field liquefaction index test that would have the following advantages over the standard penetration test (SPT):

   a) Induce stresses and deformations that are more fundamentally related to the mechanisms involved in liquefaction.

b) Exhibit greater sensitivity to the soil density, which is the most important parameter in liquefaction.

c) Exhibit better repeatability of test results.

A vane shear type device was investigated for this purpose.

2) Evaluate correlations between observed behavior of sand deposits during past earthquakes and the results of the new field liquefaction index test as well as the other currently available field tests such as SPT, cone penetration, piezometer probe, and shear wave velocity measurements. To this end, field investigations would be performed in sand deposits that have been subjected to earthquakes and for which there are adequate records of the ground acceleration and behavior of the sand deposit. The field investigation of sites subject to earthquakes should result in improved empirical correlations regardless of which field test proves to correlate better with field behavior.

Phase I of the research program, which is reported herein, concentrated on the feasibility of using a vane shear type device as a field liquefaction index test. A laboratory test cell equipped with a laboratory prototype shear vane was built to investigate the behavior of sands placed at known densities and subjected to drained and undrained vane shear loading. The laboratory vane device was instrumented to record torque, pore pressure and angular displacement. Tests were performed on two uniform fine sands, one with subrounded grains and the other with angular grains, for which extensive laboratory data are available from previous laboratory research on liquefaction. The results of the laboratory vane shear tests are presented in this report and their implications with respect to the feasibility of using a vane shear device as a field liquefaction index test are discussed.

Phase II of the research program would consist of development of a vane shear device for field use and performance of the field investigations at selected earthquake sites.

2. IN SITU TESTS

2.1 Currently Available In Situ Tests

Several existing in situ tests were considered as an alternative to the standard penetration test for investigation of liquefaction potential, e.g., cone penetration test, piezometer probe profiling, pressuremeter test and shear wave velocity measurement. Of the various in situ tests currently available, the cone penetration test and piezometer probe profiling have received the greatest attention and appear to have considerable potential as an improvement over the standard penetration test.

The cone penetration test appears to have several advantages over the SPT for use in empirical correlations with liquefaction potential, namely, greater sensitivity, better repeatability and continuous profiling. Cone penetration resistance has been correlated with liquefaction potential indirectly through correlations with SPT blowcounts and relative density (e.g., Mitchell and Gardner, 1975; Schmertmann, 1975, 1978; Douglas, et al., 1981); however, such indirect correlations offer no fundamental advantage over the original correlations with SPT. No direct correlations between the cone penetration test and liquefaction potential have been developed to date, although data is currently being assembled (e.g., Youd and Bennett, 1981; Forest et al., 1981; Zhou, 1981) which may eventually form the basis for direct correlations.

Several investigators have used a cone penetrometer with a pore pressure sensing element located at the tip to measure the pore pressures generated during penetration of the soil (e.g., Wissa et al., 1975; Schmertmann, 1978; Forest et al., 1981). This device has been called a piezometer probe. Pore pressures measured with piezometer probes in silty sands appear to be sensitive to the density of the sand, with both positive and negative pore pressures generated at the tip of the probe. These results are particularly encouraging, since they appear to permit a more fundamental interpretation of the test results in terms of the dilative/contractive behavior of the sand. When the pore pressure data are combined with the penetration resistance data from the cone itself, this device appears to have considerable potential as a liquefaction index test.

A major disadvantage of the piezometer probe is the complex state of stress at the tip. The increase in normal stress at the tip due to cavity expansion during penetration generates positive pore pressures which are superimposed on the pore pressures induced by shear strains. Thus a net positive pore pressure could be generated in a soil which actually dilates (i.e., generates negative pore pressures) during shear.

A further complication results from the effect of soil permeability on the magnitude of the measured pore pressure. This effect is due to the difference in the rate of pore pressure dissipation in soils of different permeability. Consider the following example. If the same penetration rate was used, a weakly dilative silty sand of low permeability (i.e., a soil which generates a small negative shear-induced pore pressure but has a net positive pore pressure during the penetration test because of the increase in normal stress at the tip of the probe) could give a greater positive pore pressure response than a strongly contractive clean sand of high permeability in which the positive shear-induced pore pressures are dissipated almost instantaneously. But it is the contractive clean sand which is more susceptible to liquefaction.

Another major disadvantage of the cone penetration test and the piezometer probe is that both tests are normally not performed in boreholes with conventional soil sampling. Thus, the nature of the soil in the stratum being tested must be deduced from the test results or extrapolated from adjacent borings.

The shear wave velocity of a soil deposit has been correlated with the potential for pore pressure generation under earthquake loading (Dobry et al., 1981). However, the potential for pore pressure generation may not be directly related to liquefaction. It has been shown (Castro et al., 1982) that even dense sands, which will not liquefy, could generate significant positive pore pressures during an earthquake.

2.2 Proposed Vane Shear Test

A vane shear test is proposed as an in situ test to evaluate liquefaction potential in sands. The primary advantage of the vane shear test is the ability to measure the shear resistance of the soil at large shear deformations. As discussed in Section 3, the shear resistance at large deformations, i.e., the steady state shear strength, is an important property of the soil in the analysis of liquefaction potential. Another advantage is that the vane shear test induces shear deformations in the soil without the volumetric strains that occur due to cavity expansion in the penetration tests.

Although the vane shear test is not new, the proposed application of the vane shear test in sands has not, to the writers' knowledge, been attempted previously. The vane device must be inserted into the sand with a minimum of disturbance, but must be sturdy enough to withstand relatively high stresses during insertion and rotation. Vane shear tests in sand might be either undrained or drained. The interpretation of undrained and drained vane shear tests is discussed in Chapter 5.

3. THE STEADY STATE OF DEFORMATION

3.1 Definition of Steady State

The concept of the steady state* of deformation is an extension of Casagrande's concept of "critical void ratio" (Casagrande, 1936, 1938). Poulos (1971, 1981) has described the concept as follows:

> "The steady state of deformation for any mass of particles is that state in which the mass is continuously deforming at constant volume, constant normal effective stress, constant shear stress, and constant velocity. The steady state of deformation is achieved only after all particle orientation has reached a statistically steady-state condition and after all particle breakage, if any, is complete, so that the shear stress needed to continue deformation and the velocity of deformation remain constant."

A special structure of the soil exists at the steady state which allows the soil to deform continuously at its minimum shearing resistance with no tendency for stress or volume changes. For cohesionless soils this structure has been postulated by Casagrande to be a "flow structure" (Castro, 1969; Casagrande, 1975; Poulos, 1981) in which "the particles become oriented such that the shear stress needed to continue deformation eventually reaches a constant value."

Laboratory triaxial test results (Castro, 1969, 1975; Castro et al., 1982) have shown that for a given sand: 1) the stresses in the steady state of deformation are dependent only on the void ratio and are independent of stress history and 2) at the steady state the mobilized friction angle is about equal to the friction angle determined at large strains in drained tests on contractive specimens.

3.2 Steady State Lines

Research (Casagrande, 1938; Watson, 1940; Roscoe and Schofield, 1958; Bishop et al., 1965; Castro, 1969) has demonstrated that, for a given soil, as the void ratio decreases, the shear stresses and effective normal stresses at the steady state of deformation increase. To apply steady state concepts to practical engineering problems, it has been helpful to consider the steady state line which is a graphical representation of the locus of all steady states of deformation for a particular soil.

*The term "state" refers to the description of the effective stress (shear stress and normal stress) and void ratio (or density) state of the soil.

Assuming that the effect of the intermediate normal stress is negligible, the state of a soil can be described by three parameters (an effective normal stress, a shear stress, and a void ratio or density). Thus, the graphical representation is a three-dimensional plot, which can be conveniently represented by a pair of two-dimensional plots with one common axis.

Two such sets of steady state line plots are shown in Fig. 3-1. A soil in the steady state of deformation would plot on the steady state line in both the effective normal stress and shear stress plots. For a given void ratio, the steady state shear strength and steady state effective stress are related by functions of the friction angle.

In general, any effective normal stress parameter, e.g., the effective minor principal stress, $\bar{\sigma}_3$; the effective major principal stress, $\bar{\sigma}_1$; the effective normal stress given by $1/2(\bar{\sigma}_1+\bar{\sigma}_3)$; the normal stress on the failure plane, $\bar{\sigma}_f$, and any shear stress parameter, e.g., maximum shear stress, $1/2(\sigma_1-\sigma_3)$; the principal stress difference, $\sigma_1-\sigma_3$; the shear stress on the failure plane, τ_f, may be used for the steady state plots.

As noted in the previous section, laboratory test data show that for all practical purposes the stresses in the steady state of deformation are dependent only on the void ratio. This implies that the steady state line is unique for a given soil and is independent of stress history and loading path.

3.3 Relationship to Liquefaction

Liquefaction is a phenomenon wherein a mass of soil loses a large percentage of its shear resistance when subjected to undrained monotonic, cyclic or shock loading, and flows in a manner resembling a liquid until the shear stresses acting on the mass are as low as the reduced shear resistance.

The loss in shear resistance results from a disturbance which converts the mass from a drained condition, at which it can sustain the in situ shear stresses, to an essentially undrained condition in which the shear resistance of the mass is lower than the imposed shear stresses that drive the liquefaction failure.

Upon liquefaction, the soil flows in a manner that resembles a liquid; however, its shear resistance is of a frictional nature rather than of a viscous nature, as in a true liquid. During flow the shear strength is a function of the effective stresses, which are generally not zero.

From the above description and previous discussions, it is seen that 1) liquefaction is a physical phenomenon involving

large, unidirectional deformations of soil masses and 2) the steady state of deformation is the final stage of shear during large, unidirectional continuous deformations of a soil. Thus, one would expect that during liquefaction failures the soil will tend toward the steady state of deformation. Laboratory test results (Castro et al., 1982) have shown that the steady state line is the same whether failure is initiated by monotonic or cyclic loading.

In order for a liquefaction failure to occur, the following three conditions must exist:

1. The undrained steady state strength of the soil mass must be less than the initial drained strength. This condition occurs in soils that are loose enough to generate positive pore pressures during shear (contractive behavior).

2. The driving shear stresses on the soil mass must be greater than the undrained steady state strength.

3. A triggering mechanism (e.g., an earthquake, an increase in dead load, erosion of the toe of a slope, change in seepage pressure) must occur which converts the mass from a drained condition to an essentially undrained condition of shear.

The first condition has often been used as an index criterion for evaluating the susceptibility of a soil deposit to liquefaction and will be used as such in this investigation. In general, the soil cannot liquefy if this condition (i.e., contractive behavior) does not exist. However, soils that exhibit contractive behavior cannot liquefy unless the other two conditions are also met. Thus, the condition of contractive behavior is a conservative criterion for evaluating liquefaction potential. A detailed discussion of a more rigorous analysis of liquefaction potential including the second and third conditions is presented in a previous NSF-sponsored research report (Castro et al., 1982).

In terms of the steady state plot, the first condition (undrained steady state strength less than initial drained strength) is represented by initial states that plot above the steady state line, as illustrated by point A in Fig. 3-2. In general, soils with initial states above the steady state line exhibit contractive behavior during shear (i.e., volume decrease during drained shear or development of positive pore pressures during undrained shear). Conversely, soils with initial states below the steady state line, as illustrated by point B in Fig. 3-2, exhibit dila-

tive behavior (i.e., volume increase during drained shear or development of negative pore pressures during undrained shear) and therefore have undrained steady state strengths greater than the initial drained strength.

Thus, the steady state line represents an approximate boundary between soil states that are susceptible to liquefaction (contractive behavior) and that are not susceptible to liquefaction (dilative behavior). It can be seen from the steady state plot in Fig. 3-2 that: 1) for a constant effective normal stress, susceptibility to liquefaction increases with decreasing soil density and 2) for a constant density, susceptibility to liquefaction increases with increasing effective normal stress.

4. LABORATORY INVESTIGATION

4.1 General

A laboratory investigation was performed to investigate the behavior of sands subjected to vane shear under controlled conditions. Tests were performed on two uniform fine sands, one with subrounded grains and the other with angular grains, for which extensive laboratory data is available from previous laboratory research on liquefaction (Castro et al., 1982) sponsored by NSF.

This section contains descriptions of the laboratory test apparatus, test procedure and properties of the sands tested. Results of individual tests are plotted in the appendix and the test results are discussed in Section 5.

4.2 Test Apparatus

The test apparatus consists of a K_o-consolidation cell with a shear vane located in the center of the cell. Photographs of the cell and test setup are shown in Fig. 4-1 and a cross section of the cell is shown in Fig. 4-2. The cell is made of aluminum and the shear vane is made of stainless steel.

Vertical consolidation pressure is applied by fluid pressure on a flexible rubber membrane in the bottom of the cell. The cell is sealed to permit backpressure saturation and volume change measurements during consolidation. Volume changes are measured with calibrated burettes attached to the cell drainage port at the top of the cell and the vertical pressure inlet for the rubber membrane at the bottom of the cell. The top of the cell is designed so that it can be adjusted downward inside the cell body to permit consolidation of relatively compressible materials without overextending the rubber membrane.

The cell is designed to be rigid to prevent lateral deformation and to maintain an essentially K_o condition. The theoretical radial expansion of the cell is less than 0.001% per kg/cm^2 of cell pressure and the theoretical overall volumetric expansion is less than 0.02% per kg/cm^2 of cell pressure.

The position of the shear vane is fixed by ball bearings in the cell top and base. O-ring seals are used for the pressure seals between the cell and the vane shaft. The vane shaft is surrounded by stainless steel slip rings to eliminate friction on the shaft from the surrounding soil. The total measured friction on the shaft at the maximum cell pressure of 10 kg/cm^2 was 2 in.-lbs, which corresponds to an error of 0.02 kg/cm^2 in the calculated shear stress on the vane.

The vane is rotated by hand with a handle that fits onto the top end of the vane shaft. An electronic torque transducer is attached to the handle to measure the torque applied to the vane. Two ports for measuring pore pressure are located in the body of the vane. A pore pressure transducer is mounted outside the cell at the bottom end of the vane shaft and is connected to the pore pressure ports by a duct in the shaft. Angular displacement of the vane is measured with a linear displacement transducer connected by a spring-tensioned line to a pulley mounted near the bottom of the vane shaft. The torque, pore pressure, and displacement transducer outputs are recorded on a strip chart recorder.

4.3 Description and Properties of Sands Tested

4.3.1 Banding Sand #6

Banding Sand is the trade name for a type of sand produced and sold by the Ottawa Silica Co., Ottawa, Illinois. It is derived from the St. Peter sandstone through a washing and screening process that produces a clean, uniform, fine quartz sand with subrounded grains. Scanning electron microphotographs are shown in Fig. 4-3. Commercial uses of the sand include glass making and molds for metal castings.

The gradation of Banding sand varies somewhat for different shipments. Banding Sand #6 is a designation given to a particular gradation used in a previous laboratory research program on liquefaction. The grain size curve for Banding Sand #6 is shown in Fig. 4-4.

The index properties of Banding Sand #6 are summarized in Table 4-1.

The steady state line was determined for Banding Sand #6 in a previous research program (Castro, et al., 1982) using load-controlled consolidated-undrained triaxial compression (R) tests. Steady state lines in terms of effective normal stress on the failure surface, $\bar{\sigma}_f$, and shear stress on the failure surface, τ_f, are presented in Figs. 4-5 and 4-6. An average steady state line from the laboratory tests is shown along with a band indicating the scatter of the laboratory data. The effective stress friction angle from the $\bar{R}$-tests was approximately 30° over most of the range of densities tested.

4.3.2 Mine Tailings Sand

The mine tailings sand was obtained from a copper mining operation in Highland Valley, British Columbia. The tailings sand is a uniform, fine sand, almost entirely quartz, with angu-

lar grains. Scanning electron microphotographs are shown in Fig. 4-3.

The grain-size curve for the mine tailings sand is shown in Fig. 4-4 and the index properties of the sand are summarized in Table 4-1.

The steady state lines for the mine tailings in terms of effective normal stress on the failure surface, $\bar{\sigma}_f$, and shear stress on the failure surface, τ_f, are shown in Figs. 4-7 and 4-8. The effective stress friction angle from the $\bar{R}$-tests was approximately 32° over most of the range of densities tested.

4.4 Test Procedure

4.4.1 Sample Preparation

Sand was compacted inside the cell with the vane in place. The sand was mixed to a water content of 5% and compacted in layers using a tamping method. The compaction effort, number of layers and number of coverages per layer were varied for each test to achieve the target density. The loosest samples were compacted in 8 layers using a static weight. For tests at intermediate densities, a spring-loaded static tamper was used and the samples were compacted in 8 to 12 layers. The densest samples were compacted in 12 layers using a small pneumatic hammer. The same compaction foot was used for all samples. The shape of the compaction foot is designed to fit in between the fins of the shear vane, as shown in Fig. 4-2.

After compaction of the last layer, the upper part of the cell body (which serves as a compaction collar) was removed and the top of the soil was trimmed flush with the top of the cell. The upper part of the cell body and cell top were then fastened to the cell and water was circulated upward through the sample under gravity flow to saturate the sand.

4.4.2 Backpressure Saturation

After saturation by gravity flow, an initial vertical confining pressure of 0.25 kg/cm^2 was applied and the sample was backpressure saturated. Backpressure saturation was performed by simultaneously increasing the vertical confining pressure applied by the pressure membrane and the backpressure applied through the cell drainage port. The backpressure was raised in increments of 1 kg/cm^2, allowing water to enter the sample and equalize before applying the next increment. After several backpressure increments were applied, the Skempton B-value was checked by increasing the vertical pressure applied by the rubber membrane and monitoring the pore pressure response of the sample with the pore

pressure transducer attached to the shear vane. A backpressure of 9.00 kg/cm^2 (the maximum backpressure for which the equipment was designed) was used in all tests. This backpressure generally resulted in a B-value of 0.90 or greater.

4.4.3 Consolidation

After backpressure saturation, the samples were consolidated to an effective vertical stress of 1 kg/cm^2. Volume changes during consolidation were measured by 1) measuring the volume of water entering the vertical pressure inlet for the rubber membrane at the bottom of the cell and 2) measuring the volume of water exiting the sample through the cell drainage port. The volume changes from both measurements were generally in good agreement.

4.4.4 Shear

A handle equipped with a torque transducer was fit onto the end of the shear vane shaft which extends through the cell top. Using this handle, the vane was rotated by hand at approximately constant velocity while the torque, pore pressure, and angular displacement were recorded on a strip chart recorder. Rotation was continued until the shear resistance (torque) leveled off at a constant value with increasing angular displacement, i.e., until a steady state of deformation was achieved.

Undrained loading was attempted in Test No. 1, and the cell drainage was kept closed during this test in order to measure the equalized pore pressure in the cell after the test. All other tests were drained. In the drained tests, the cell drainage was left open during shear and the rate of shear was kept slow enough so that no excess pore pressure was measured with the pore pressure sensor in the shear vane.

Additional shear trials were performed after the initial shearing in each test. In general, the peak and steady state shear resistances in subsequent trials were different than in the first trial. In most of the tests, additional trials were performed until the steady state shear resistance remained the same in two or more consecutive trials.

In several tests, cyclic shear was applied to the vane after the steady state shear resistance had leveled off with additional trials. The cyclic shear consisted of typically about 20 to 40 cycles applied at a rate of about 0.5 to 1 cycle/sec with a stress amplitude of about 0.10 to 0.20 kg/cm^2 along the failure surface. Generally no induced pore pressures were recorded during cyclic shear indicating that the cyclic portion of the test was drained. In Test No. 8 a small induced pore pressure

(0.02 kg/cm^2) was measured indicating that this test was not completely drained during cyclic shear. The cyclic shear was then followed by an additional trial with unidirectional shearing.

5. DISCUSSION OF TEST RESULTS

5.1 General

Seven vane shear tests were performed on Banding Sand #6 and four tests were performed on Mine Tailings Sand. The test apparatus, test procedure, and properties of the sands tested are described in Section 4.

For each sand, the individual test specimens were compacted to initial densities above and below the steady state line. The positions of the consolidated states of the individual specimens with respect to the steady state line are shown in Fig. 5-2 for tests on Banding Sand #6 and in Fig. 5-3 for tests on Mine Tailings Sand. The results of individual tests are plotted in the appendix in terms of shear stress versus circumferential displacement.

This secion contains a discussion of the test results. Conclusions with respect to the feasibility of the proposed vane shear test as an in situ index test for evaluation of liquefaction potential are presented in Section 6.

5.2 Undrained Vane Shear Test

Ideally, it would be desirable to perform an undrained vane shear test in the field, since the soil undergoes essentially undrained shear during liquefaction. An undrained test with measurement of the shear-induced pore pressure would permit a direct evaluation of liquefaction potential in terms of the steady state concepts discussed in Section 3.3.

For an undrained test to be feasible, the rate of pore pressure dissipation must be slow enough to permit measurement of the shear-induced pore presssures at practical rotation rates for a vane shear device.

An undrained test was attempted in Test No. 1 on Banding sand. The steady state of deformation was reached in approximately 2 sec. in this test. The cell drainage was kept closed during the test in order to measure the difference between the peak shear-induced pore pressure measured at the vane and the equalized pore pressure in the cell after the test. The pore pressure measured at the vane during shear did not exhibit a peak followed by a drop off due to dissipation. Rather, the pore pressure appeared to equalize throughout the cell almost instantaneously, i.e., the shear deformation in the failure zone occurred under essentially drained conditions except for the gradual buildup of an equalized pore pressure in the cell due to the fact that the cell drainage was closed.

Based on this initial test, it was concluded that an undrained test was not practical in a clean fine sand, and the remainder of the test program was directed toward establishing the feasibility of a drained vane shear test.

5.3 Drained Vane Shear Tests

The stress strain curves obtained from the drained vane shear tests are presented in the appendix. In general, the shear stress reached a peak in each trial and then decreased. The deformations were continued until the shear stress (i.e., the torque) reached a constant value with increasing deformation (steady state).

The results of the drained vane shear tests are summarized in Fig. 5-1. The measured peak and steady state shear stresses for the first trial are plotted as a function of the initial void ratio after consolidation. Two reference lines are shown on the plots: 1) the steady state void ratio, e_{ss}, at the initial effective normal stress on the failure surface, $\bar{\sigma}_f$, and 2) the drained steady state shear strength, τ_{ss}, computed assuming that there is no change in $\bar{\sigma}_f$ during shear (e.g., as would be measured in a drained direct shear test). In the following discussions the values of e_{ss} and τ_{ss} are referred to as the reference steady state void ratio and reference steady state shear stress, respectively. The initial effective normal stress on the failure surface (i.e., the horizontal effective normal stress after consolidation) was computed assuming $K_o = 0.5$. Since all tests were performed with a vertical consolidation stress of 1 kg/cm^2, the computed initial effective normal stress on the failure surface was 0.5 kg/cm^2 for all tests. The reference steady state void ratio at this stress was obtained from the steady state line determined from triaxial tests (Figs. 4-5 and 4-7). The estimated value of the reference drained steady state shear strength at the initial effective normal stress was computed using the effective stress friction angle from the $\bar{R}$ triaxial tests (it could also be obtained directly from the steady state plots in terms of shear stress, Figs. 4-6 and 4-8).

As shown in Fig. 5-1, the measured shear stresses plot below the reference steady state shear stress (τ_{ss} reference line) at high void ratios (low initial densities). With decreasing void ratio (increasing density) the measured shear stresses increase abruptly to values well above the reference steady state shear stress. This abrupt increase occurs at void ratios somewhat lower than the reference steady state void ratio (e_{ss} reference line). In order to understand the behavior shown in Fig. 5-1, it is helpful to look at the test results in terms of the state diagram.

Steady state plots in terms of effective normal stress are presented in Fig. 5-2 for the tests on Banding Sand #6 and in Fig. 5-3 for the tests on Mine Tailings. The steady state points for the vane shear tests were obtained as follows: 1) the effective normal stress on the failure surface at the steady state was calculated from the measured steady state shear stress using the effective stress friction angle determined from the $\bar{R}$ triaxial tests and 2) the void ratio in the shear zone at the steady state was obtained by assuming that the steady state point for the vane shear test lies on the steady state line determined from the triaxial tests.

As shown in the steady state plots, effective stress changes occurred in the shear zone during the drained vane shear tests. The effective stress changes are due to a complex interaction between the volume changes in the shear zone and the stress strain characteristics of the soil surrounding the shear zone. The test results can be interpreted in terms of steady state concepts as follows:

1. When the initial state of the soil is above the steady state line (i.e., loose), the soil in a thin shear zone around the vane contracts. As the soil in the shear zone contracts, a reduction in the horizontal effective normal stress in the shear zone occurs due to arching in the surrounding soil (e.g., Test No. 5 in Fig. 5-2). As a result of this effective stress reduction, the drained steady state shear strength measured in the vane shear test with arching is less than the reference steady state shear strength (i.e., as measured in a drained direct shear test without arching). Thus, the steady state shear stress measured in the vane shear test plots below the τ_{ss} reference line in Fig. 5-1.

2. Conversely, when the initial state of the soil is below the steady state line, the soil in the shear zone dilates, resulting in an increase in the effective normal stress in the shear zone (e.g., Test No. 4 in Fig. 5-2). In this case, the drained steady state shear strength measured in the vane shear test is greater than the reference drained steady state shear strength (i.e., as measured in a direct shear test without this "reverse" arching). Thus, the steady state shear stress measured in the vane shear test plots above the τ_{ss} reference line in Fig. 5-1.

The behavior described above was observed for tests with initial states above the steady state line and for tests with

initial states well below the steady state line. However, for initial dilative states slightly below the steady state line, the test results indicate a decrease in effective normal stress instead of the increase that one could have expected for dilative states. In the tests on Banding Sand #6, this deviation from the expected behavior occurred when the initial state was less than about 0.06 below the steady state line in terms of void ratio (this is equivalent to 20% in terms of relative density and 3% in terms of percent compaction according to ASTM D-1557). This deviation from the expected behavior occurred over a greater range of densities in the Mine Tailings, when the initial state was less than about 0.17 below the steady state line in terms of void ratio (42% in terms of relative density and 7% in terms of percent compaction).

One possible explanation for this deviation from the expected trend is as follows. Dilative soils generally undergo a slight initial contraction at the beginning of shear deformation, resulting in an initial reduction of the effective normal stress. Thus the soil surrounding the shear zone undergoes a rebound and reload cycle as the soil in the shear zone first contracts and then dilates. If inelastic deformation occurs in the surrounding soil during this rebound-reload cycle, the soil in the shear zone must dilate past the initial void ratio in order to increase the effective normal stress back to the initial value. Thus, if the inelastic deformation of the surrounding soil during rebound-reload is of sufficient magnitude, a weakly dilative soil might experience a net reduction in effective normal stress due to arching.

Another possible explanation for the deviation from the expected results described above is that the steady state lines determined from the triaxial tests are in error (i.e., located too high in the state diagram in Figs. 4-5 through Fig. 4-8) due to the strain limitations of the triaxial test. Although the possibility of some error due to the strain limitations of the triaxial test has been recognized (Castro et al., 1982), it appears unlikely that this error could be large enough to explain the deviation observed for the Mine Tailings.

Factors such as grain breakage, dilative-contractive behavior (Poulos, 1981) or other factors that have not been identified could also cause or contribute to this deviation from the expected behavior.

The deviation from the expected behavior discussed above leads to a conservative interpretation of the test results, i.e, slightly dilative soils might be classified as being susceptible to liquefaction. The degree of conservatism introduced by this deviation appears to vary for different soils and needs to be investigated further.

The test results summarized in Fig. 5-1 indicate that the peak shear stress may be a practical and less conservative alternative to the steady state shear stress as an index of liquefaction potential in a drained vane shear test. The behavior observed in drained triaxial and direct shear tests indicates that the peak shear stress would generally be about the same as the steady state shear stress in uncemented loose sands and greater than the steady state shear stress in dense sands. This relationship appears to be confirmed by the vane shear tests. Since the variation of the peak shear stress with void ratio is similar to the variation of the steady state shear stress with void ratio, the interpretation of a drained vane shear test in terms of the measured peak shear stress would be similar to the interpretation in terms of the steady state shear stress.

In Fig. 5-1 the peak shear stress becomes equal to the reference steady state strength at void ratios that are only slightly lower than the reference steady state void ratio. The difference in void ratio is about 0.04 for Banding sand, which is equivalent to a difference of 14% in terms of relative density and a difference of 2% in terms of percent compaction according to ASTM D-1557. For mine tailings the corresponding differences are 0.07 in void ratio, 18% in relative density and 3% in percent compaction. These differences are considered to be small for practical applications, and thus the comparison of peak shear stress with the reference steady state strength appears to provide a good basis for relating the state of the soil in situ to its steady state.

Two trends were noted in the test results that may provide additional methods of interpreting the results of drained vane shear tests. It was noted that for initial states above the steady state line (i.e., contractive states), the shear stress measured in the first trial tended to be lower than the shear stress measured in subsequent trials. Conversely, for initial states below the steady state line (i.e., dilative states), the shear stress measured in the first trial tended to be greater than the shear stress measured in subsequent trials. This trend was stronger for the peak shear stress than for the steady state shear stress. The ratio of peak shear stress in the second trial to that in the first trial is plotted versus void ratio in Fig. 5-4. The ratio is less than one for both sands at initial states denser than the reference void ratio, e_{ss}, with the exception of Test 2 in which the initial state is very close to the steady state line.

In several tests, mostly on mine tailings, a cyclic shear stress was applied after completing several monotonic applications of shear. A monotonic test was performed after the cyclic shearing and the peak shear stress after cyclic shearing was com-

pared with the peak shear stress measured in the first trial, as shown in Fig. 5-5. For both Banding sand and mine tailings at initial states substantially denser than the steady state, the post cyclic peak strength was lower than the initial peak strength, indicating a loosening effect of the cyclic deformations accompanied by arching.

6. CONCLUSIONS

6.1 Conclusions from Laboratory Investigation

The laboratory test results indicate that a vane shear test can be used to evaluate the susceptibility of sands to liquefaction.

An undrained vane shear test does not appear to be practical due to rapid dissipation of the shear-induced pore pressures. It may be possible to obtain partially drained pore pressure data in clean sands by locating the pore pressure measuring device closer to the shear zone, and an essentially undrained test may be feasible in silty sands. However, it appears that a drained vane shear test holds greater promise for a field device.

A drained vane shear test can be used to evaluate the liquefaction potential of sands based on the effective stress changes that occur in the shear zone during the test. The effective stress changes are due to a complex interaction between the volume changes in the shear zone and the stress-strain characteristics of the soil surrounding the shear zone. These stress changes result in changes in the measured shear stress that are sensitive to variations in soil density and that can be interpreted in terms of steady state concepts.

The complex interaction that produces the effective stress changes in a drained shear test is affected by factors such as soil compressibility, gradation and grain shape (which affect the magnitude of shear induced volume changes), grain breakage, overconsolidation and cementation. Additional laboratory investigation is required to evaluate the influence of these factors on the test results.

The test results obtained in the present laboratory investigation suggest that a drained vane shear test could be interpreted as follows. A reference drained steady state shear stress, τ_{ss}, corresponding to zero change in effective normal stress, is computed from $\tau_{ss} = \sigma_f \tan \phi$. The initial effective normal stress on the failure surface of the vane, σ_f, is estimated from an analysis of the in situ stresses at the test location. For level ground, σ_f can be estimated using a reasonable value for the at rest earth pressure (e.g., $K_o = 0.5$ for a normally consolidated deposit). A reasonable estimate of the friction angle (e.g., $\phi = 30°$ to $35°$) is also required. If the peak shear stress measured in the vane shear test is less than the reference value, τ_{ss}, the initial state lies above the steady state line and the soil is considered susceptible to liquefaction. Conversely, if the measured peak shear stress is greater than the

reference value, the initial state lies below the steady state line and the soil is not susceptible to liquefaction.

The laboratory test results indicate that the above interpretation would be somewhat conservative, since the peak shear stress measured in tests at densities slightly below the steady state line were actually lower than the reference value. However, for the two sands tested the degree of conservatism is considered to be reasonable for pratical applications. The degree of conservatism in other sands needs to be investigated further.

Trends were noted in the results of subsequent shear trials following the first trial which may provide additional methods of test interpretation. The peak shear stress in the second trial and the peak shear stress after cyclic shearing tended to be greater than the peak shear stress in the first trial for initial states above the steady state line and lower than the first trial peak for initial states below the steady state line.

6.2 Nature of Field Device

The vane device must be inserted into the sand with a minimum of disturbance but must be sturdy enough to withstand relatively high stresses during insertion and rotation. It is unlikely that these requirements could be met with a vane configuration similar to the standard shear vane used in clays. In order to meet the strength requirements, the vane device would probably consist of anywhere from 6 to 12 short fins mounted on a cylindrical body. In order to minimize disturbance during insertion into the soil, the vane could be designed as a "self-boring" device using equipment and techniques similar to those developed for the self-boring pressuremeter. Baguelin and Jezequel (1975) report on a self-boring vane device called a "self-boring shearmeter" developed in France. A design consisting of short vanes mounted on a hollow thin-wall cylinder that can be pushed into the soil might also be feasible.

It would be desirable to instrument a prototype field device with a pore pressure transducer. The pore pressure measuring system could be used for controlling the rate of vane rotation to ensure drained conditions in silty sands, as well as for possible performance of undrained or partially drained tests. It may be possible to eliminate the pore pressure transducer for drained tests by developing criteria for vane rotation rates in various soils. Blight (1968) has developed a theoretical approach that could be used to preselect rotation rates for drained vane shear tests in silty sands.

In summary, the design of a field vane shear device for drained tests in sands would be significantly different and more

complex than existing shear vanes used in clays. Nevertheless, a practical field device appears to be feasible with existing field test equipment technology.

ACKNOWLEDGEMENTS

We gratefully acknowledge the assistance of Dr. Robert Lo of Klohn-Leonoff Consultants, Ltd. in obtaining the mine tailings sample used in the testing program. Drs. Ronald C. Hirschfeld and Steve J. Poulos provided valuable input into the conduct of the investigation. John L. Enos ably performed the laboratory tests.

REFERENCES

Baguelin, F., and Jezequel, J. F. (1975) "Further Insights on the Self-Boring Technique Developed in France," Proceedings, Conference on In-situ Measurement of Soil Properties, ASCE, Raleigh, NC, Vol. 2, pp. 231-241.

Bishop, A. W., Webb, D., and Skinner, A. E. (1965) "Triaxial Tests on Soils at Elevated Cell Pressures," Proceedings 6th ICSMFE, Vol. 1, pp. 170-174, Montreal.

Blight, G. E. (1968) "A Note on Field Vane Testing of Silty Soils," Canadian Geotechnical Journal, Vol. 5, No. 3, pp. 142-149.

Casagrande, A. (1936) "Characteristics of Cohesionless Soils Affecting the Stability of Slopes and Earth Fills," Boston Society of Civil Engineers, Oct. 1940. Originally published in the Journal of the Boston Society of Civil Engineers, Jan. 1936.

Casagrande, A. (1938) "The Shearing Resistance of Soils and its Relation to the Stability of Earth Dams," Proceedings, Soils and Foundation Conference of the U.S. Engineer Department.

Casagrande, A. (1975) "Liquefaction and Cyclic Deformation of Sands, A Critical Review," Proceedings, 5th Panamerican Conference on Soil Mechanics and Foundation Engineering, Vol. 5, pp. 79-133, Buenos Aires, Argentina.

Castro, G. (1969) "Liquefaction of Sands," PhD Thesis, Harvard Soil Mechanics Series, No. 81, Pierce Hall, Harvard University.

Castro, G. (1975) "Liquefaction and Cyclic Mobility of Saturated Sands," Journal of the Geotechnical Engineering Division, ASCE, Vol. 101, No. GT6, pp. 551-569.

Castro, G.; Poulos, S. J.; France, J. W. and Enos, J. L. (1982) "Liquefaction Induced by Cyclic Loading," Report Submitted to National Science Foundation, Contract No. PFR-7924731.

Dobry, R.; Stokoe, K. H.; Ladd, R. S. and Youd, T. L. (1981) "Liquefaction Susceptibility from S-Wave Velocity," Insitu Testing to Evaluate Liquefaction Susceptibility, Proc. of Session No. 24, ASCE National Convention, St. Louis, Missouri.

REFERENCES
(continued)

Douglas, B. J.; Olsen, R. S., and Martin, G. R. (1981) "Evaluation of the Cone Penetremeter Test for SPT-Liquefaction Assessment," Insitu Testing to Evaluate Liquefaction Susceptibility, Proc. of Session No. 24, ASCE National Convention, St. Louis, Missouri.

Forrest, J. B.; Ferritto, J. M. and Wu, G. (1981) "Site Analysis for Seismic Soil Liquefaction Potential," Proceedings, International Conference on Recent Advances in Geotechnical Earthquake Engineering and Soil Dynamics, St. Louis, Missouri, Vol. I, pp. 155-160.

Mitchell, J. K and Gardner, W. S. (1975) "In Situ Measurement of Volume Change Characteristics," Proceedings, Conference on In Situ Measurement of Soil Properties, ASCE, Raleigh, N.C., Vol. 2, pp. 279-345.

Poulos, S. J. (1971) The Stress-Strain Curves of Soils, Geotechnical Engineers Inc., Winchester, Mass., pp. 1-80.

Poulos, S. J. (1981) "The Steady State of Deformation," Journal of the Geotechnical Engineering Division, ASCE, Vol. 107, No. GT5, pp. 553-562.

Roscoe, K. H. and Schofield, A. N. (1958) "On the Yielding of Soils," Geotechnique, Vol. VII, pp. 25-53.

Schmertman, J. H. (1975) "Measurement of In Situ Shear Strength," Proceedings, Conference on In Situ Measurement of Soil Properties, ASCE, Raleigh, N.C. Vol. 2, pp. 57-138.

Schmertman, J. H. (1978) Guidelines for Cone Penetration Test Performance and Design, Federal Highway Adminstration Research Report No. FHWA-TS-78-209.

Schmertman, J. H. (1978) "Study of Feasibility of Using Wissa-Type Piezometer Probe to Identify Liquefaction Potential of Saturated Fine Sands," Technical Report S-78-2, U.S. Army, Waterways Experiment Station, Vicksburg, Mississippi.

Seed, H. B. and Idriss, I. M. (1981) "Evaluation of Liquefaction Potential of Sand Deposits Based on Observations of Performance in Previous Earthquakes," Insitu Testing to Evaluate Liquefaction Susceptibility, Proc. of Session No. 24, ASCE National Convention, St. Louis, Missouri.

REFERENCES
(concluded)

Watson, J. D. (1940) "Stress Deformation Characteristics of Cohesionless Soils from Triaxial Compression Tests," ScD. Thesis, Pierce Hall, Harvard University.

Wissa, A. E. Z.; Martin, R. T. and Garlanger, J. E. (1975) "The Piezometer Probe," Proceedings, Conference on In Situ Measurement of Soil Properties, ASCE, Raleigh, N.C., Vol. 1, pp. 536-545.

Youd, T. L. and Bennett, M. J. (1981), "Liquefaction Site Studies Following 1979 Imperial Valley Earthquake," Insitu Testing to Evaluate Liquefaction Susceptibility, Proc. of Session No. 24, ASCE National Convention, St. Louis, Missouri.

Zhou, S. G. (1981) "Influence of Fines on Evaluating Liquefaction of Sands by CPT," Proceedings, International Conference on Recent Advances in Geotechnical Earthquake Engineering and Soil Dynamic, Vol. 1, pp. 167-172, St. Louis, Missouri.

TABLES

TABLE 4-1 - INDEX PROPERTIES FOR BANDING SAND #6 AND MINE TAILINGS SAND

		Banding Sand #6	Mine Tailings
D_{50}		0.157 mm	0.256 mm
Uniformity Coefficient, $C_u = D_{60}/D_{10}$		1.70	2.71
Minimum Density by ASTM 2049	e_{max} $\gamma_{d_{min}}$	0.82 91.2 pcf	1.08 80.4 pcf
Maximum Density by ASTM 2049	e_{min} $\gamma_{d_{max}}$	0.52 109.2 pcf	0.62 99.5 pcf
Maximum Density by ASTM D1557 (Compaction Test)	e_{min} $\gamma_{d_{max}}$	0.55 107.2 pcf	0.65 101.5 pcf
Specific Gravity of Solids		2.66	2.68
Grain Shape		Subrounded	Angular

FIGURES

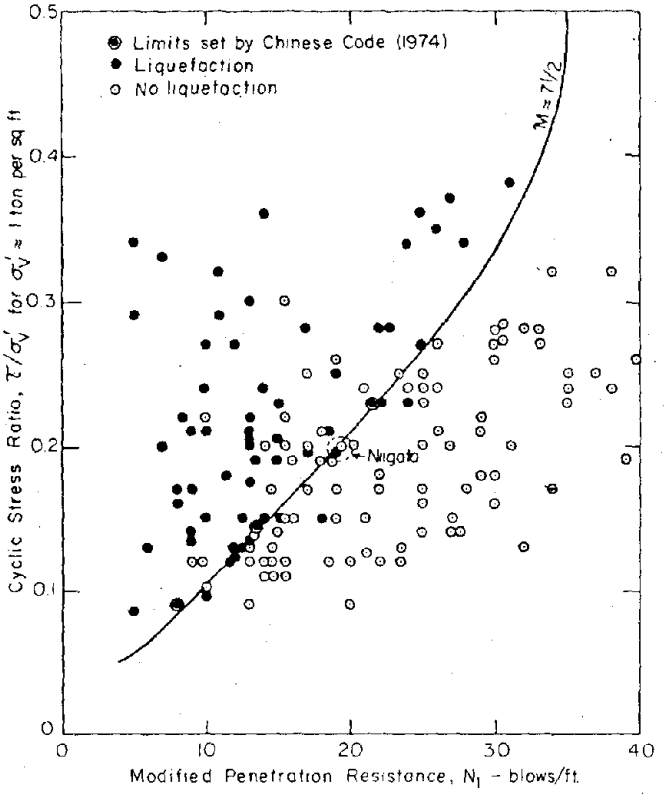

Fig. 1-1: Correlation Between Blowcounts in Sands and Earthquake Induced Ground Failure (from Seed and Idriss, 1981)

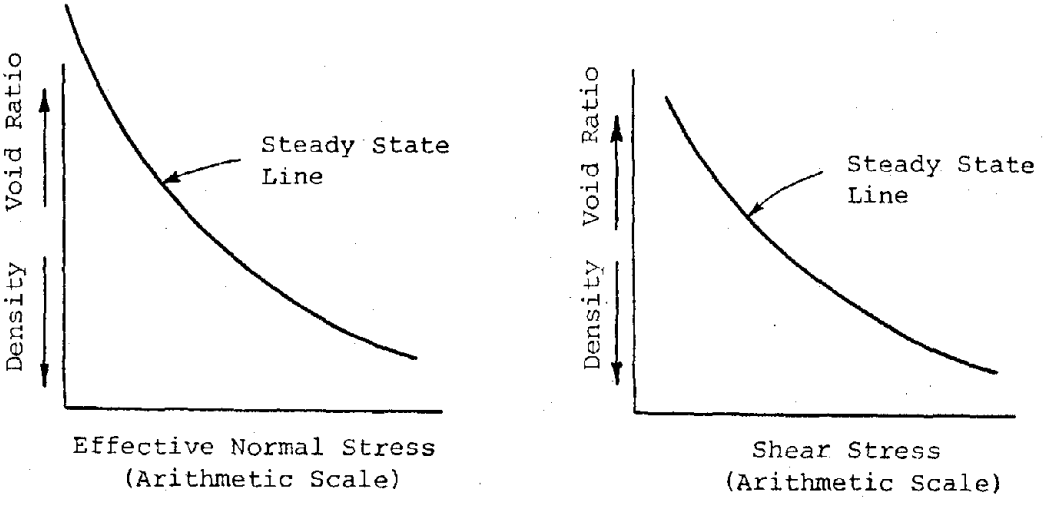

a) Steady State Lines in Arithmetic Plots

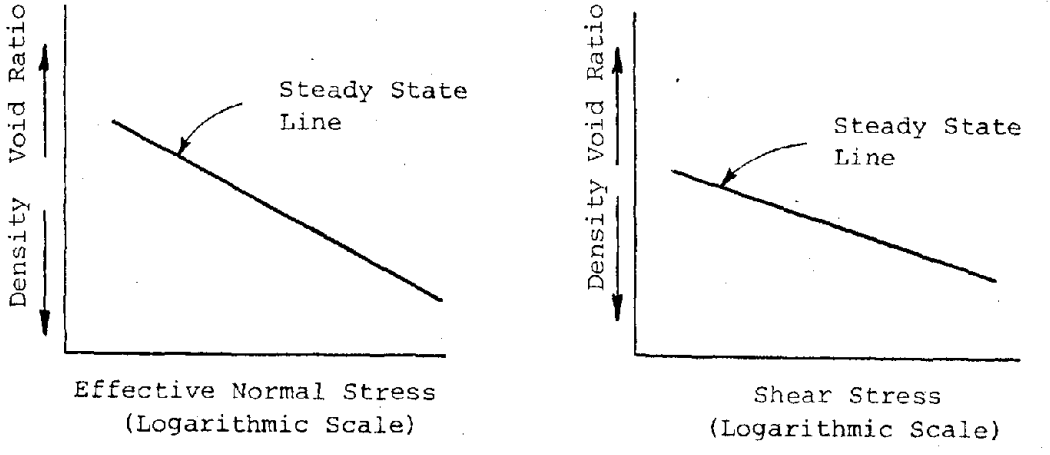

b) Steady State Lines in Semi-Logarithmic Plots

Fig. 3-1: Examples of Steady State Line Plots

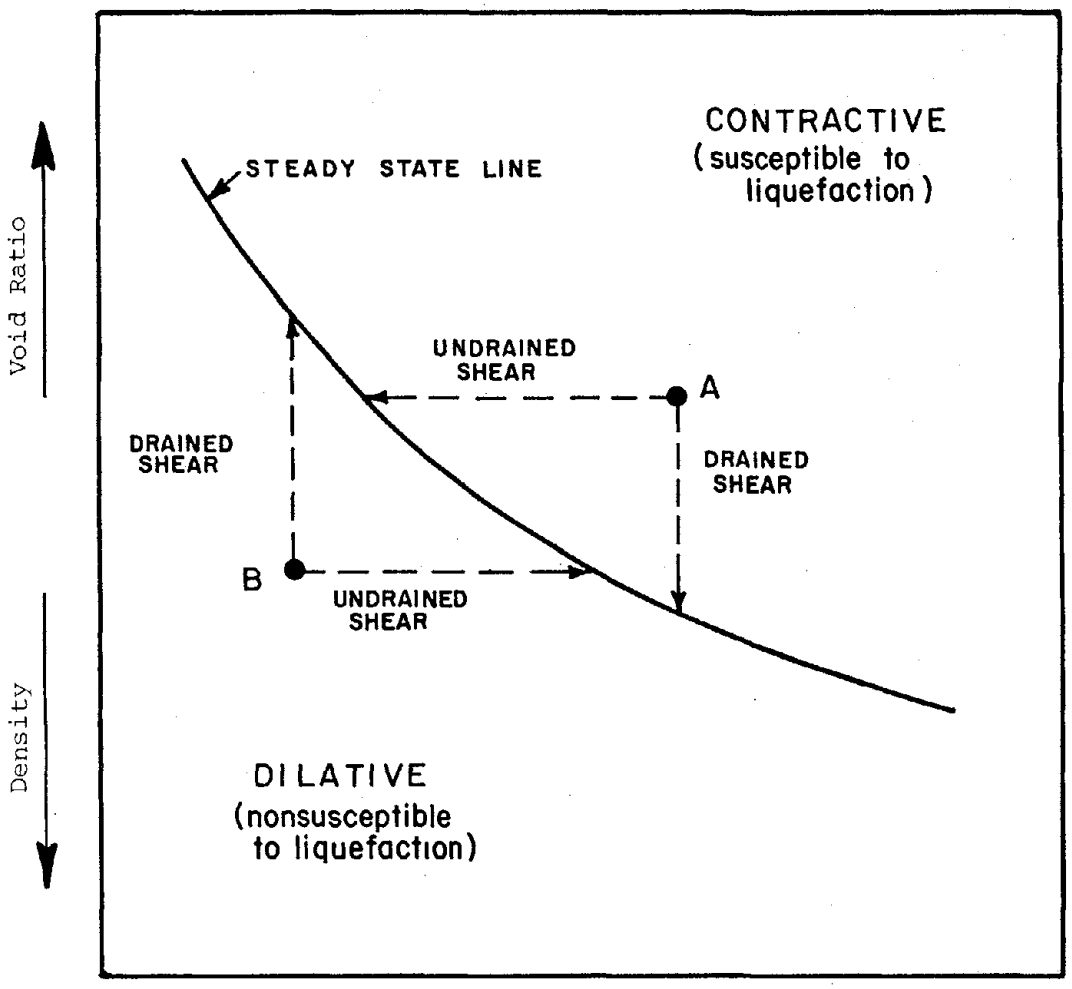

Fig. 3-2: Relationship Between Initial State and Liquefaction Potential

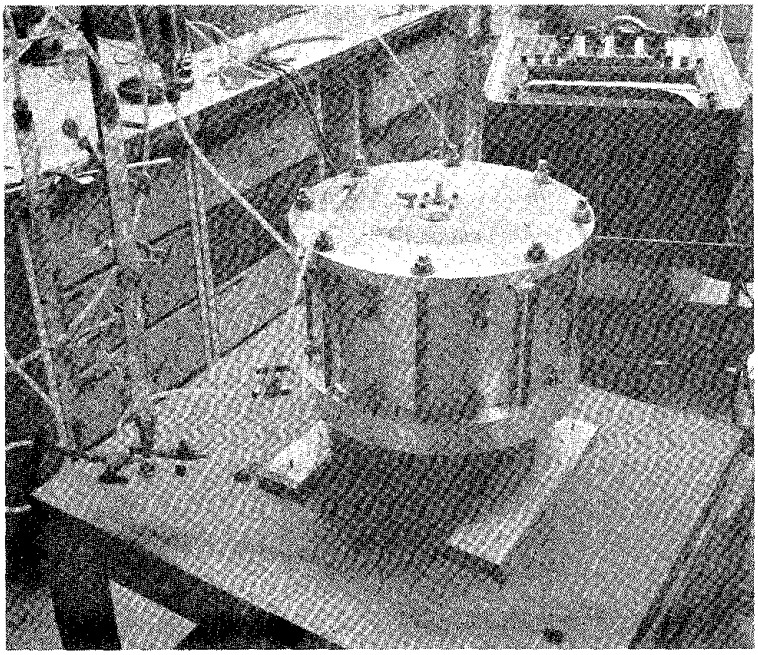

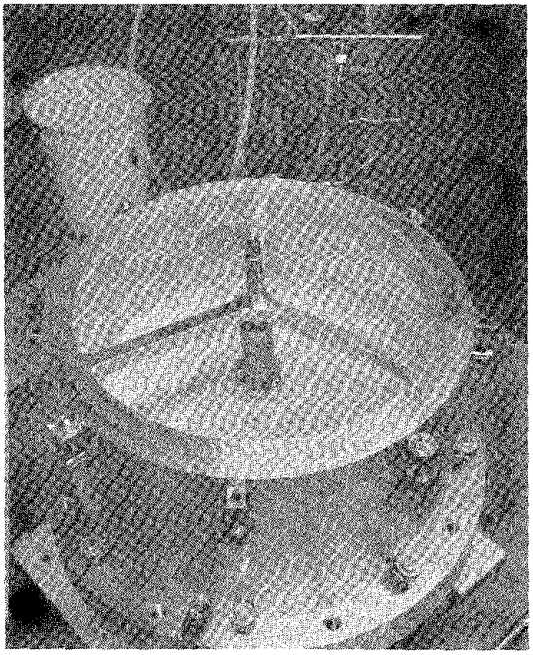

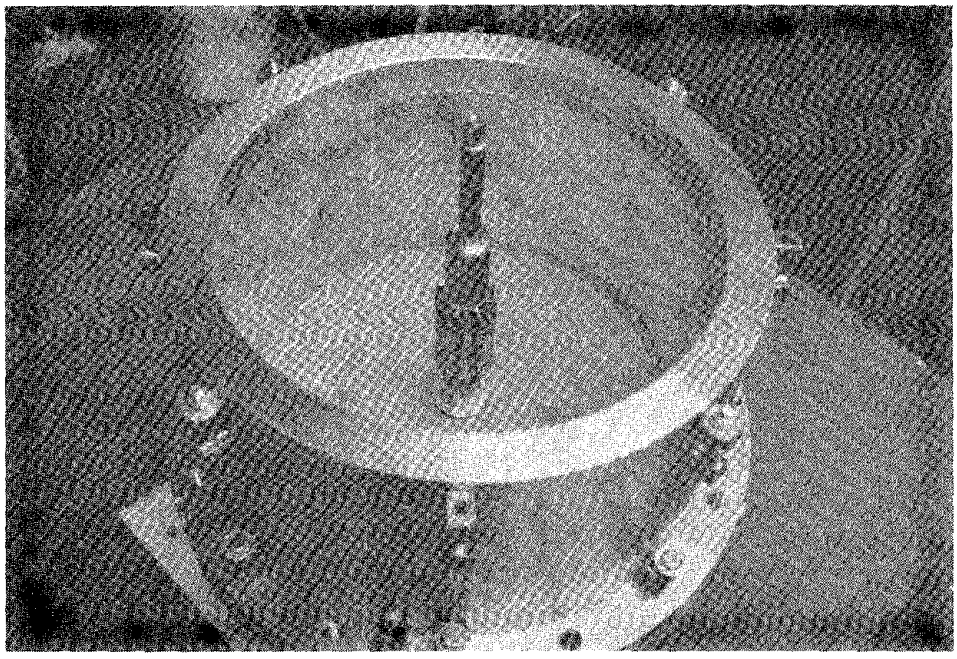

Fig. 4-1 Photographs of Test Apparatus

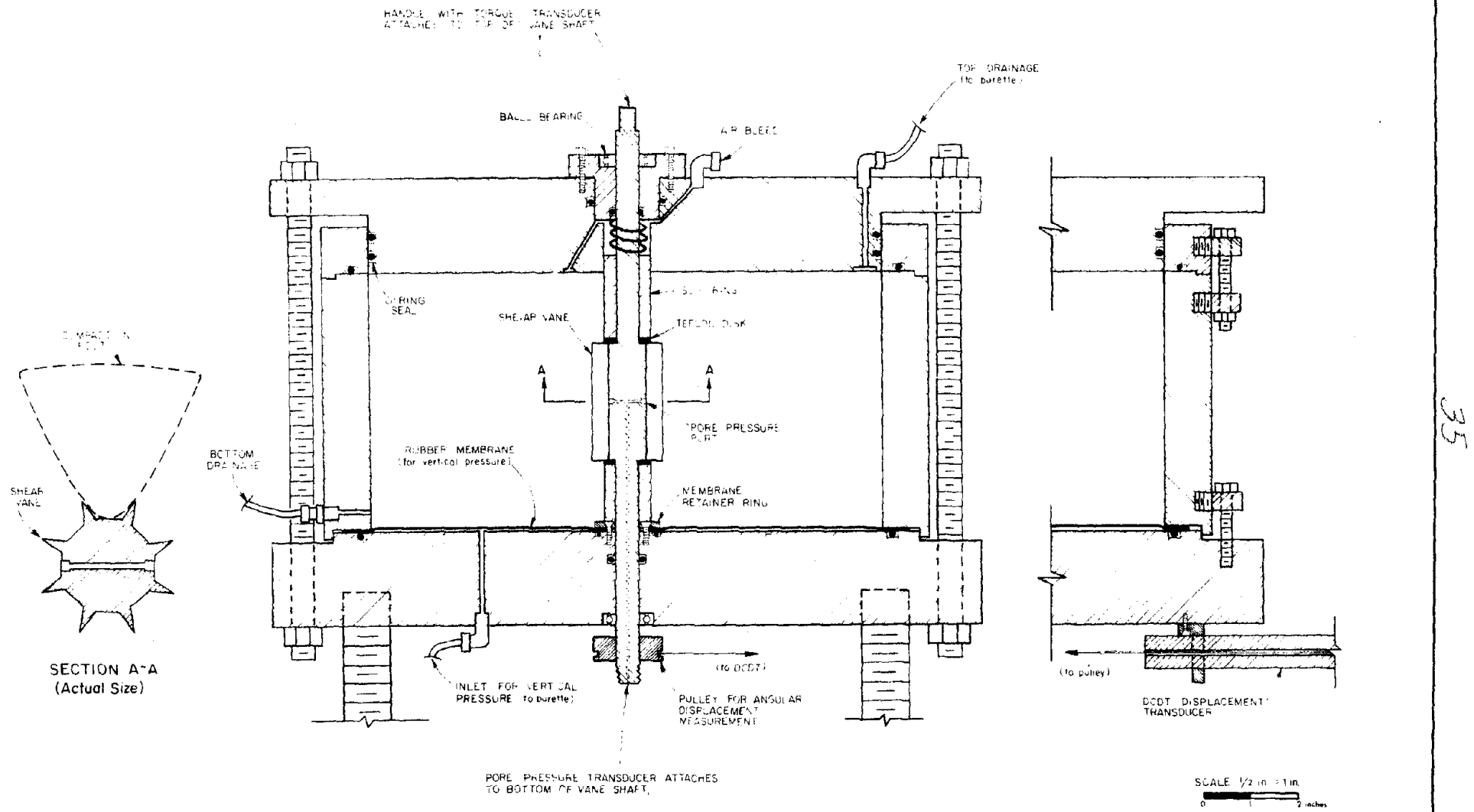

FIG. 4-2 - TEST APPARATUS

BANDING SAND

0.10 mm

BANDING SAND

0.10 mm

MINE TAILINGS

0.10 mm

MINE TAILINGS

0.10 mm

FIG. 4-3 – SCANNING ELECTRON MICROPHOTOGRAPHS

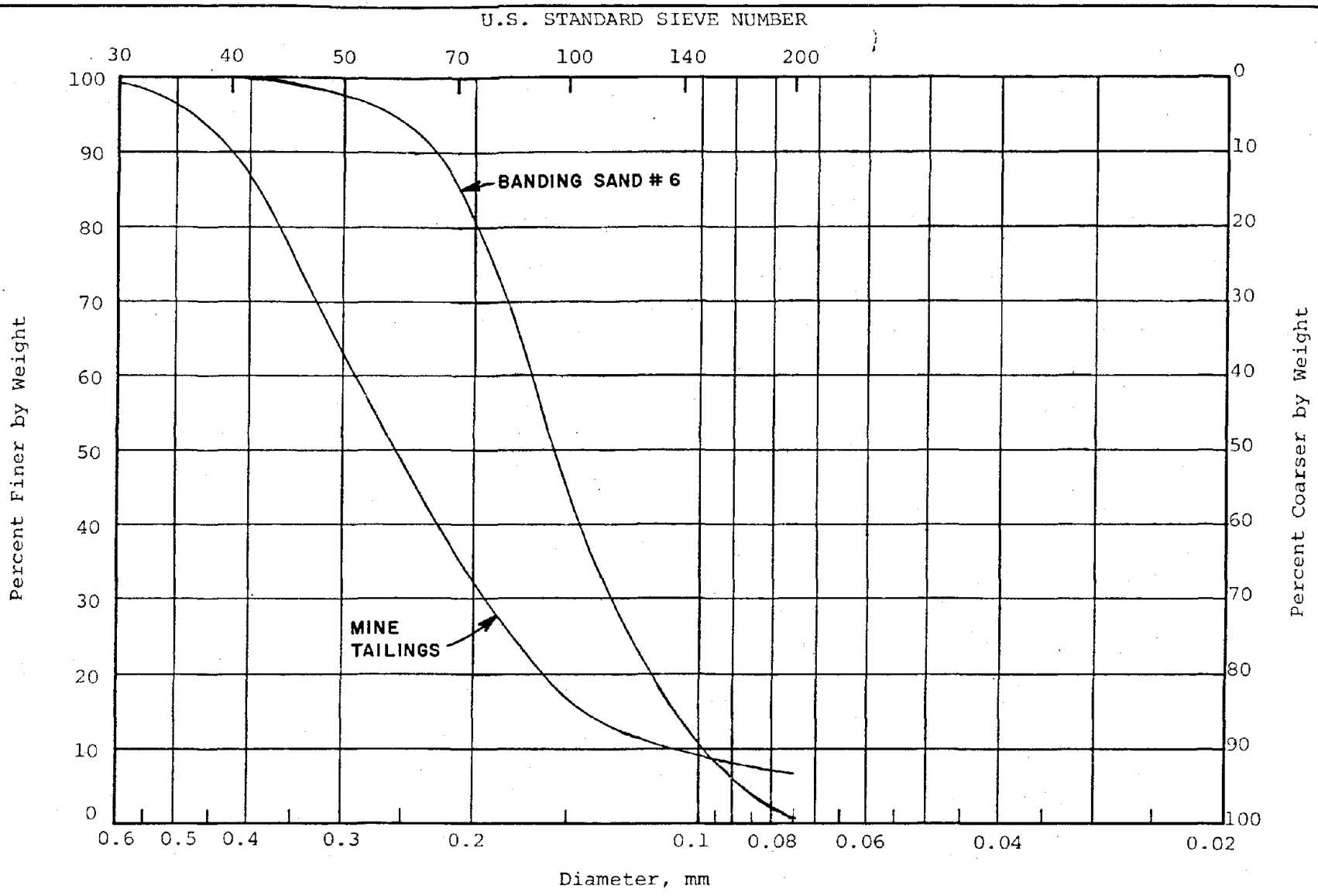

Fig. 4-4 Grain Size Curves for Banding Sand and Mine Tailings

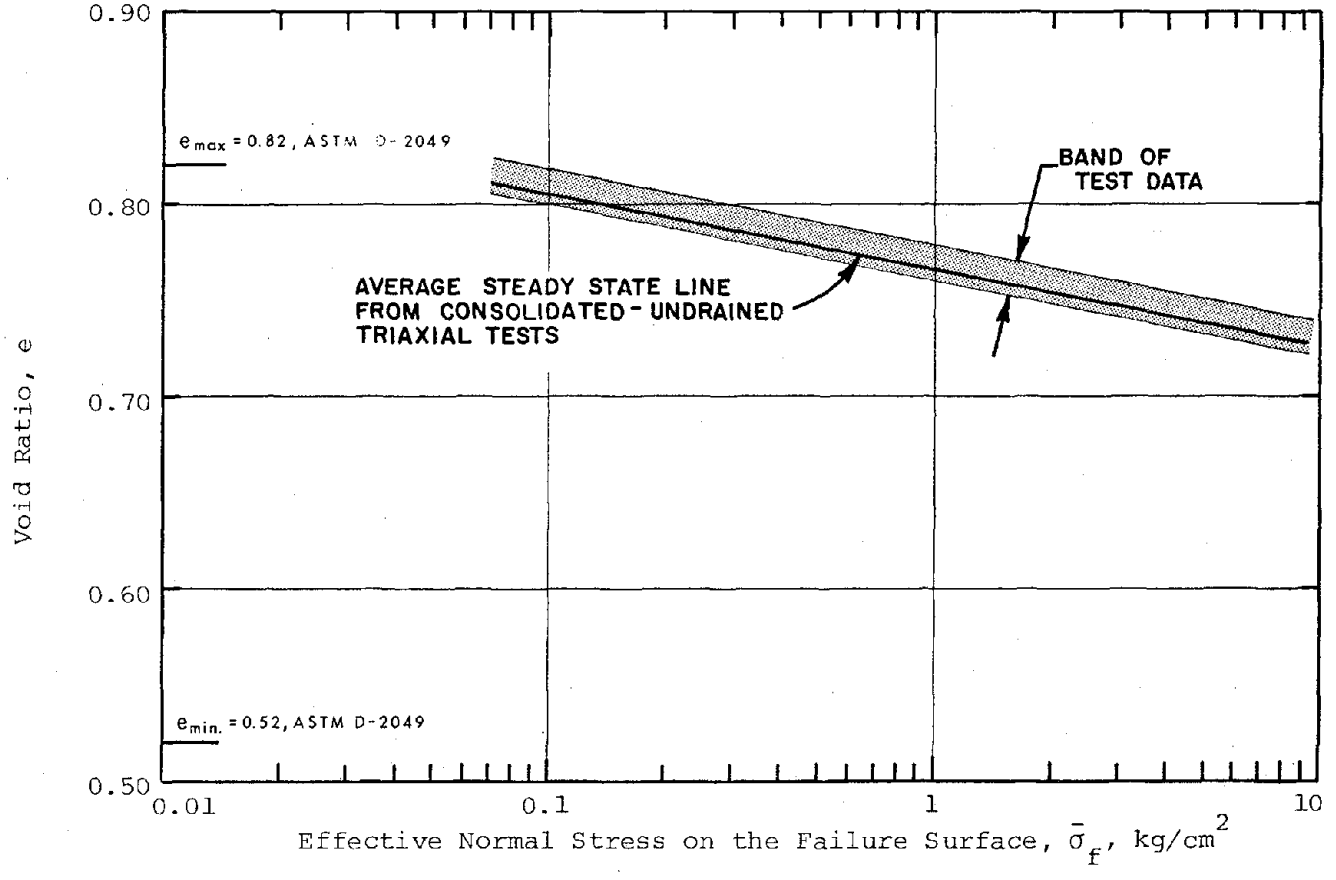

Fig. 4-5: Steady State Line for Banding Sand #6 in Terms of e vs $\bar{\sigma}_f$

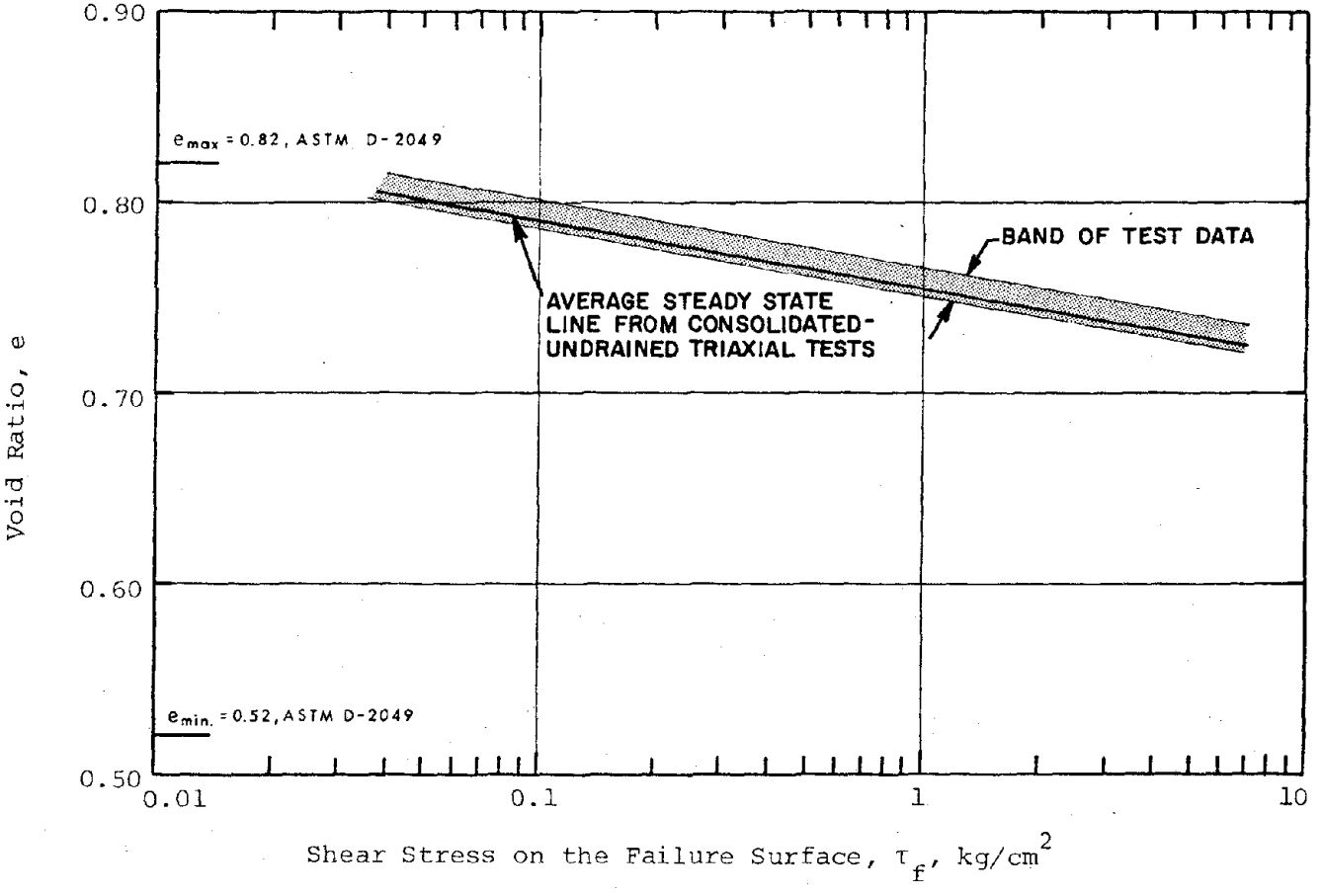

Fig. 4-6: Steady State Line for Banding Sand #6 in Terms of e vs τ_f

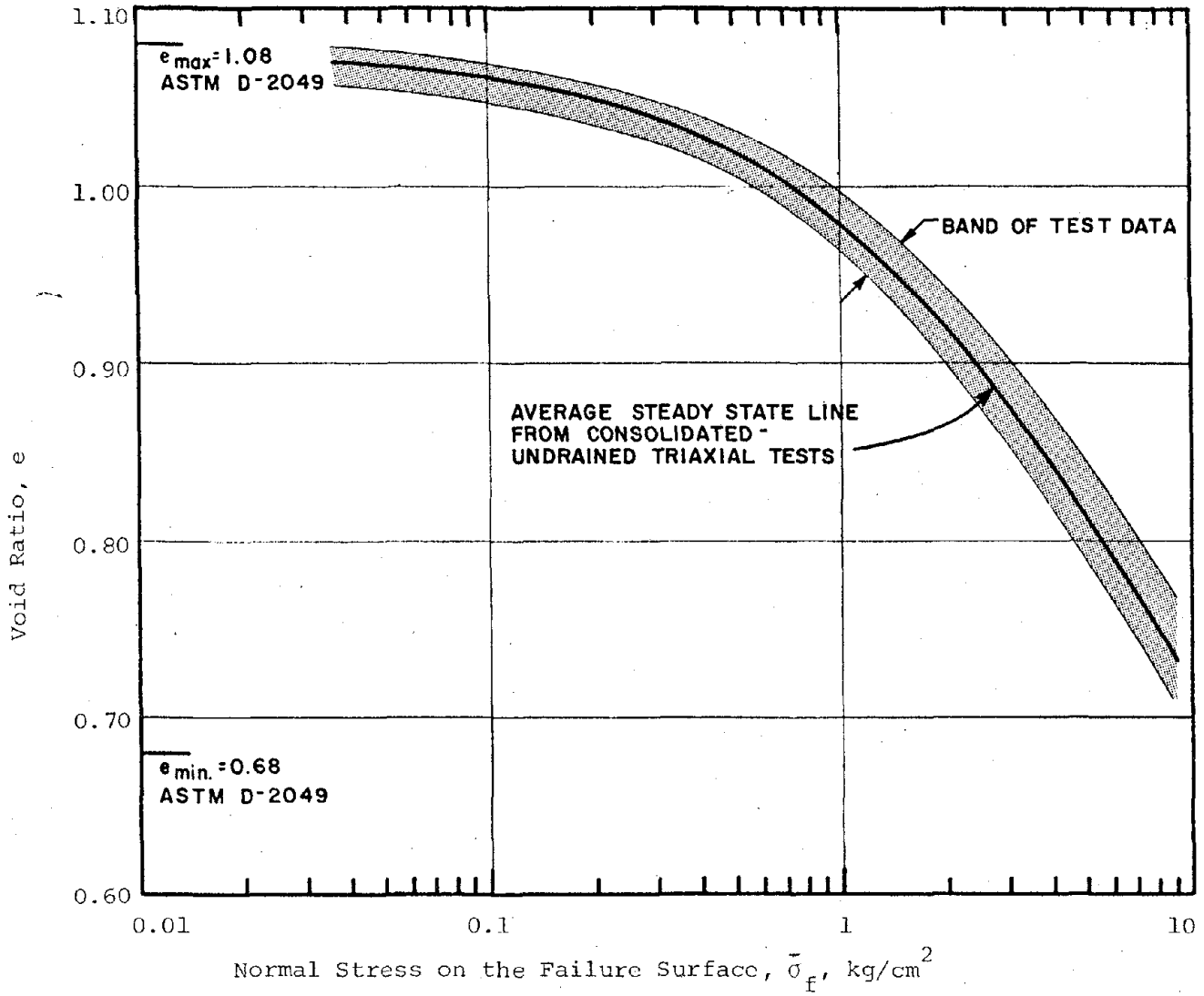

Fig. 4-7: Steady State Line for Mine Tailings Sand in Terms of e vs $\bar{\sigma}_f$

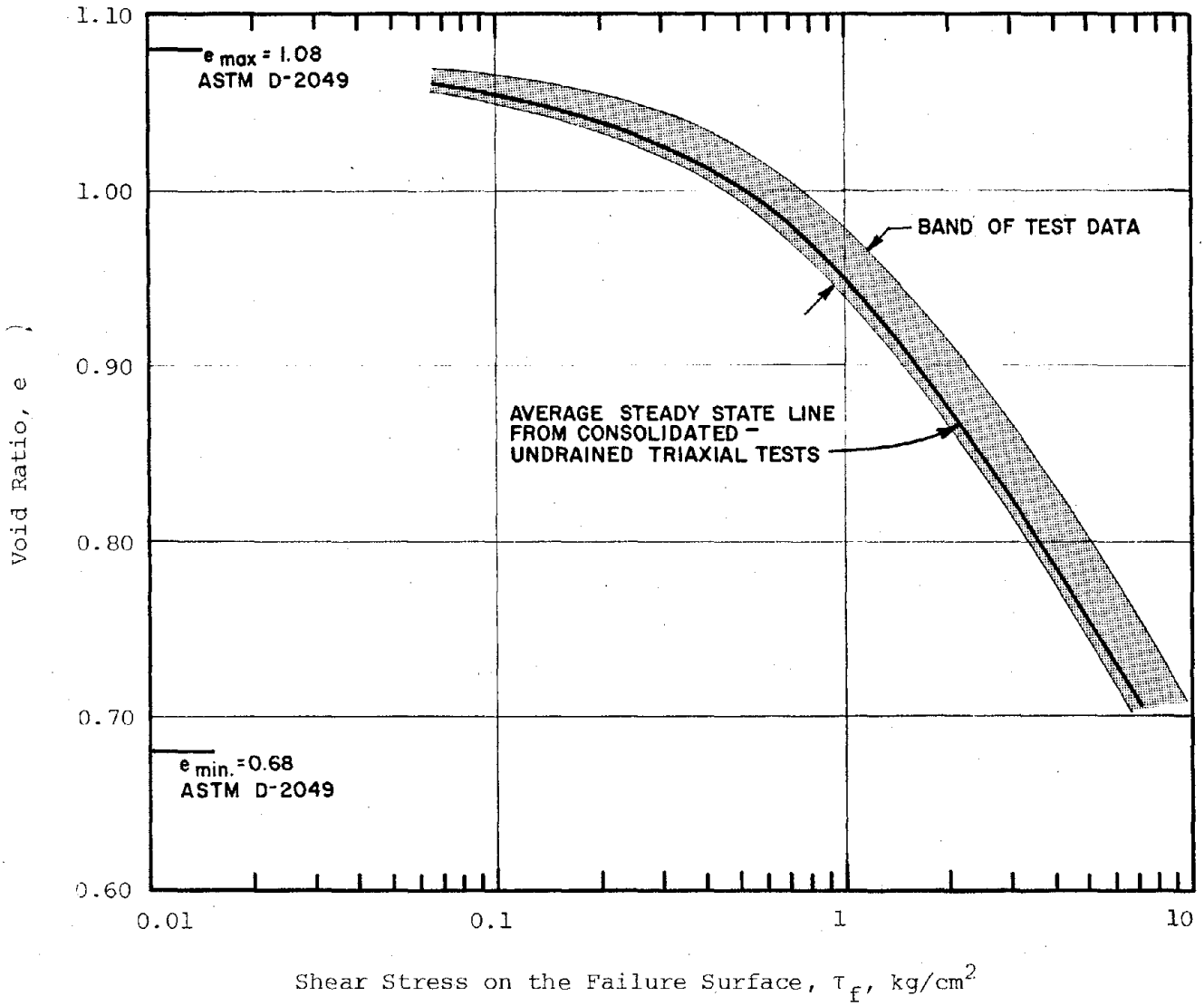

Fig. 4-8: Steady State Line for Mine Tailings Sand in Terms of e vs τ_f

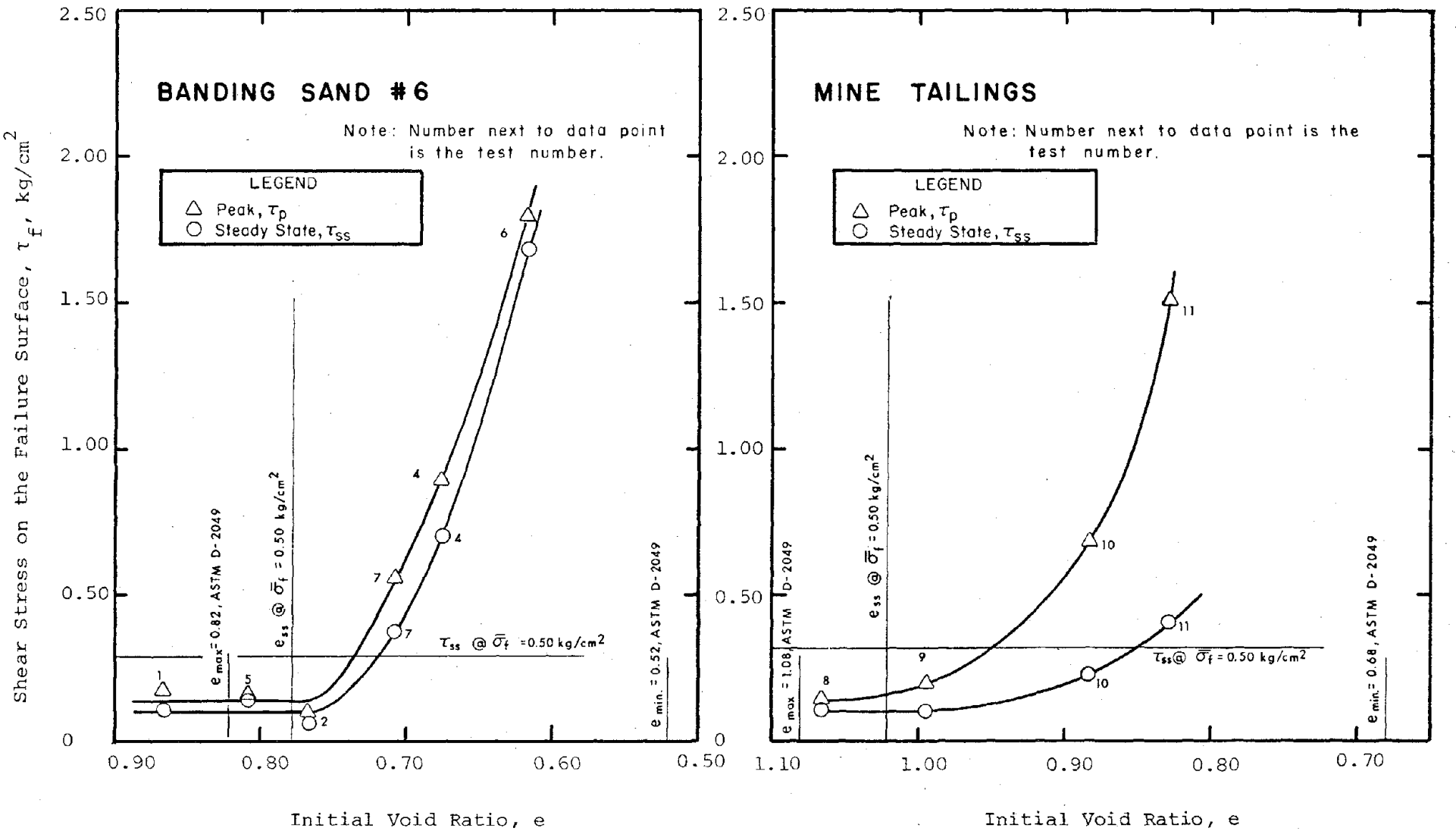

Fig. 5-1: Summary of Drained Vane Shear Test Results for First Trial

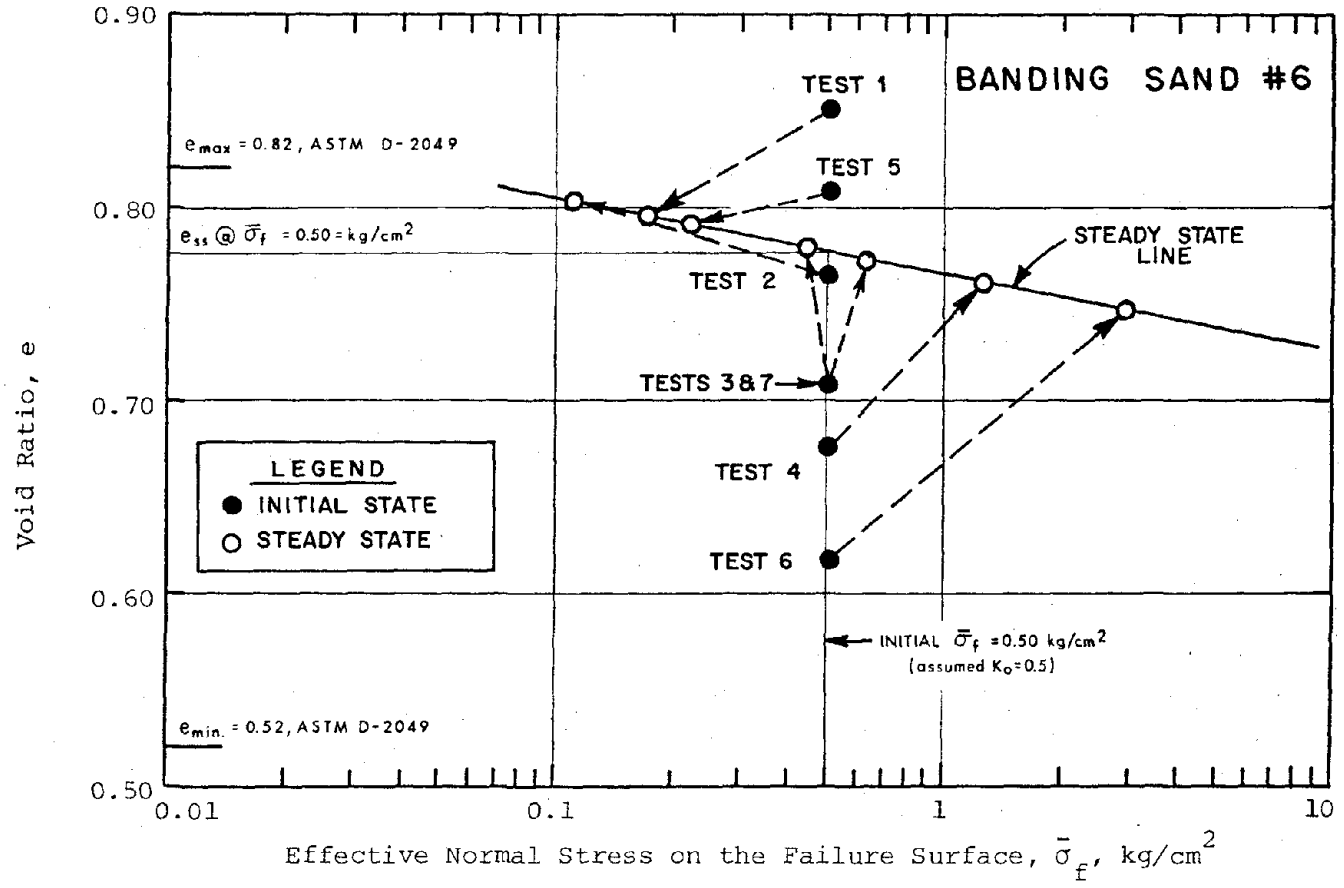

Fig. 5-2: Steady State Plot for Drained Vane Shear Tests on Banding Sand #6

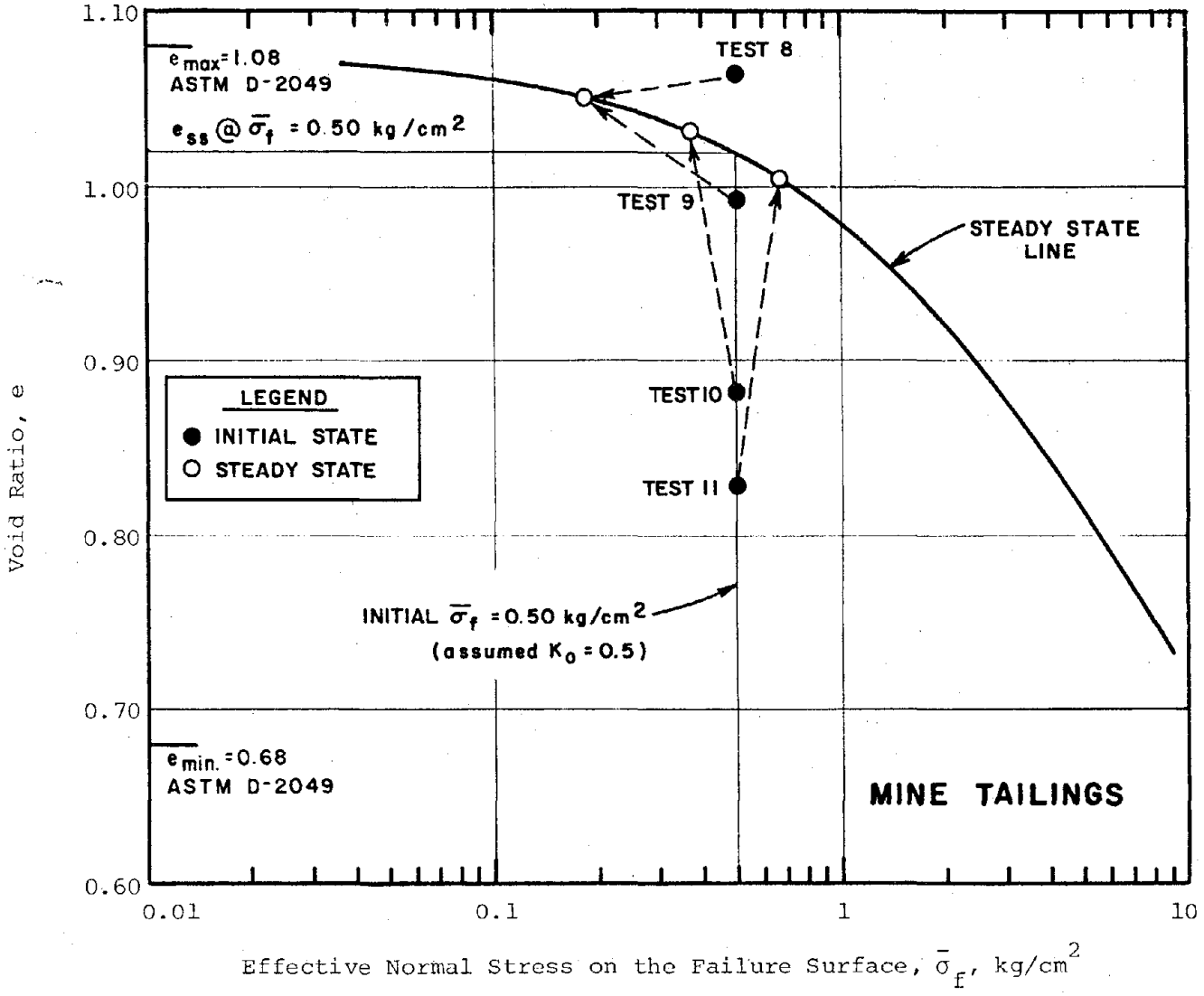

Fig. 5-3: Steady State Plot for Drained Vane Shear Tests on Mine Tailings Sand

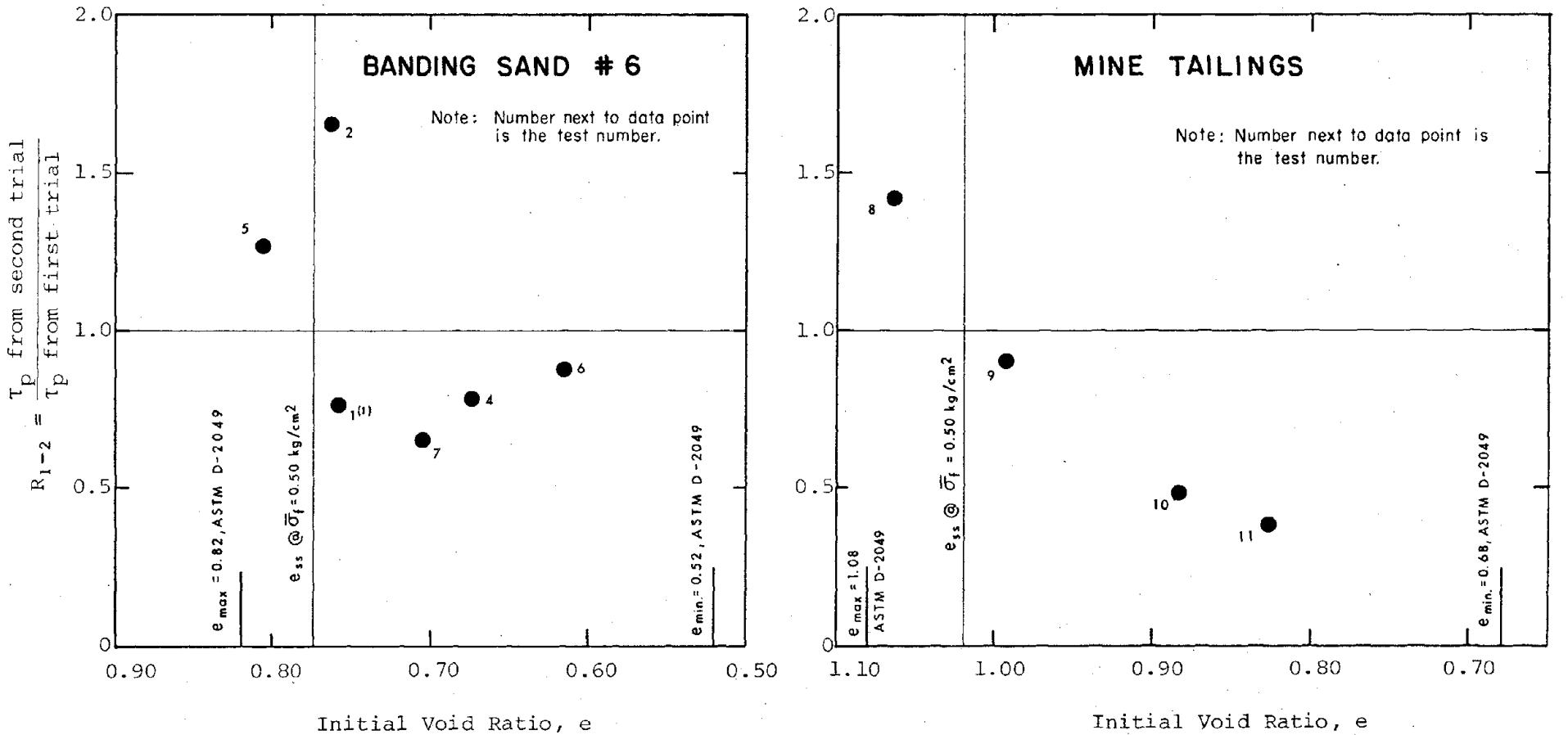

Fig. 5-4: Ratio of Peak Shear Stress from Second Trial to Peak Shear Stress from First Trial

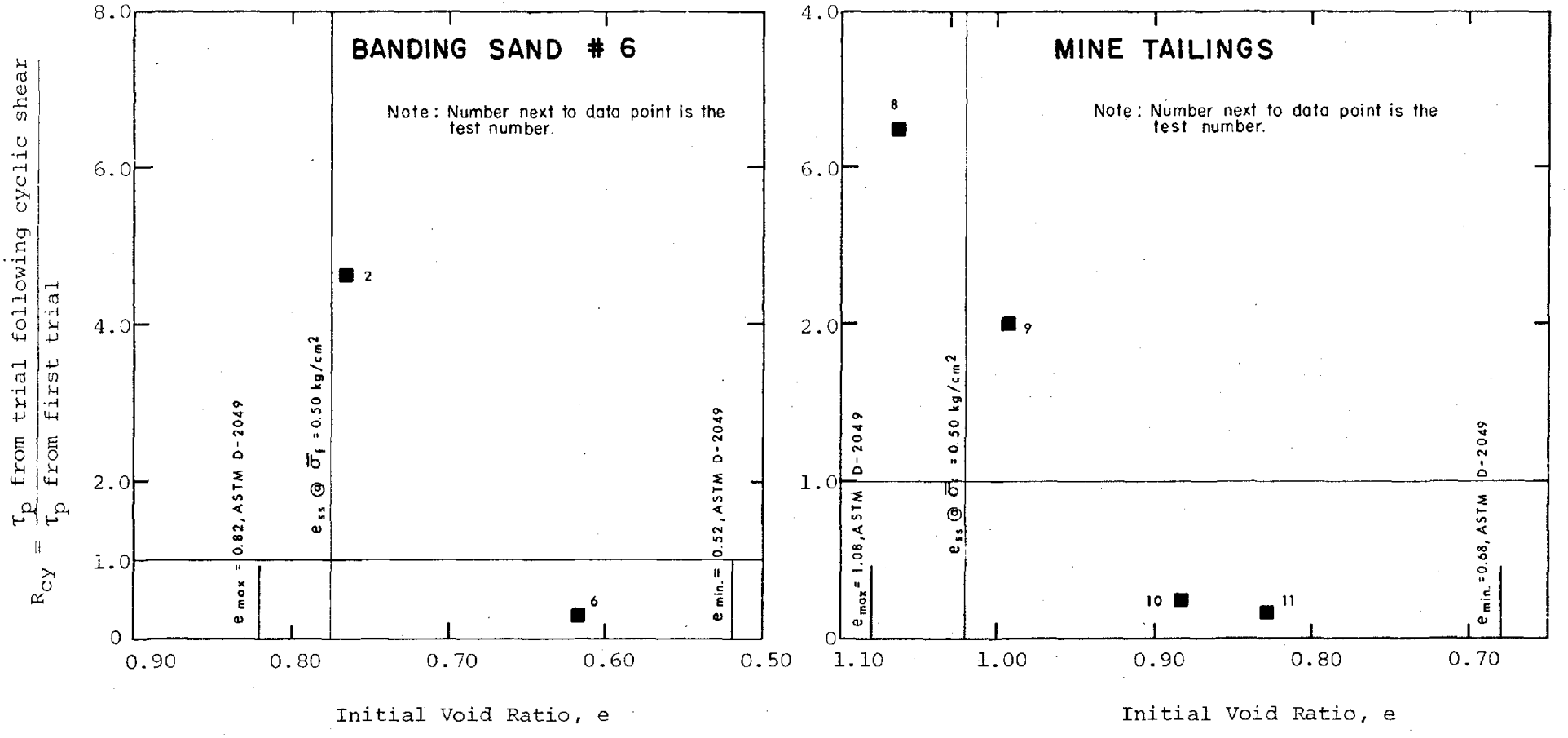

Fig. 5-5: Ratio of Peak Shear Stress Following Cyclic Shear to Peak Shear Stress from First Trial

APPENDIX

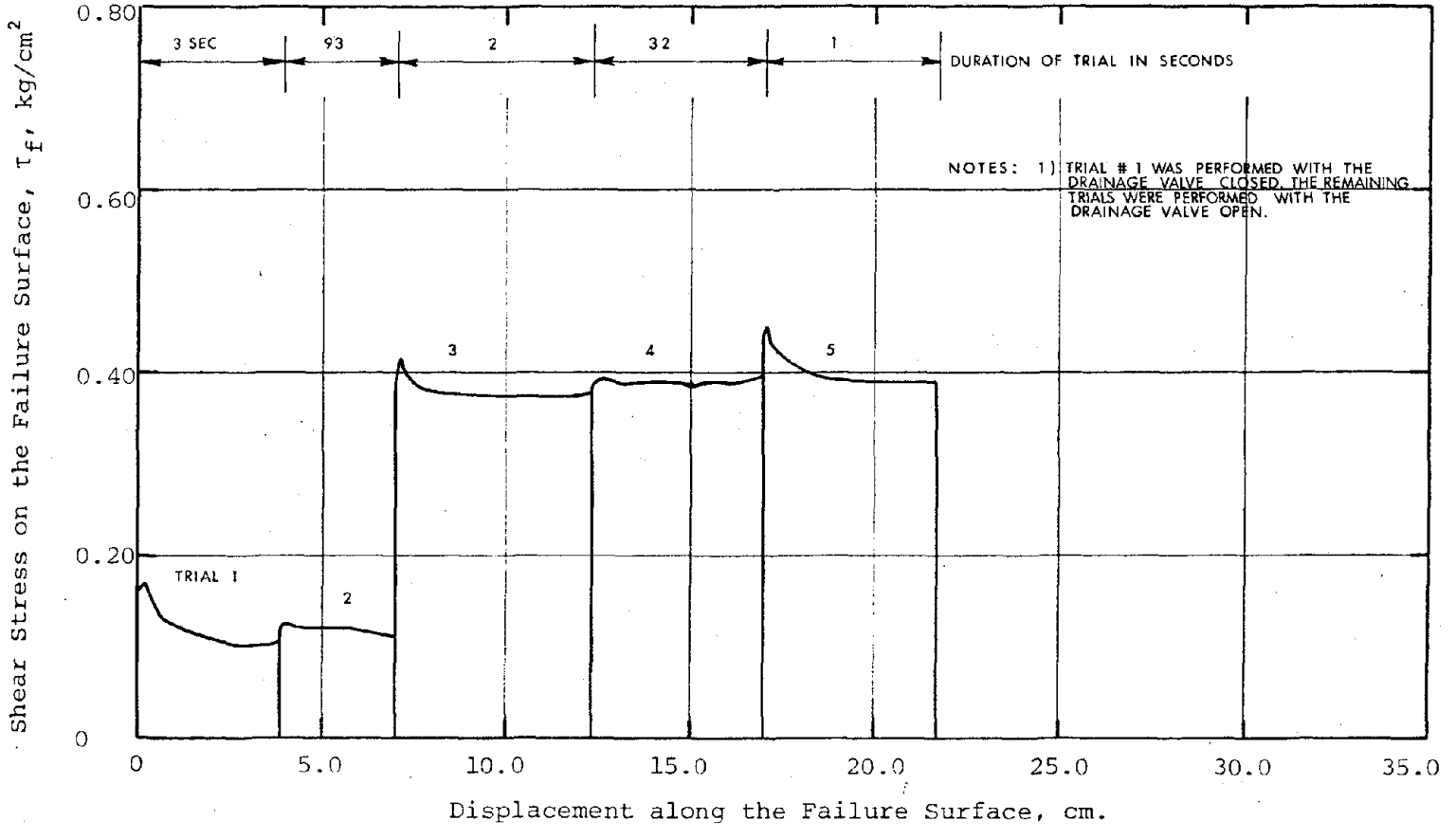

Test No. 1

Material: Banding Sand #6

State after Consolidation: $\bar{\sigma}_v = 1.00$ kg/cm^2

$e_c = 0.86$

Method of Loading: Attempted Undrained Vane Shear

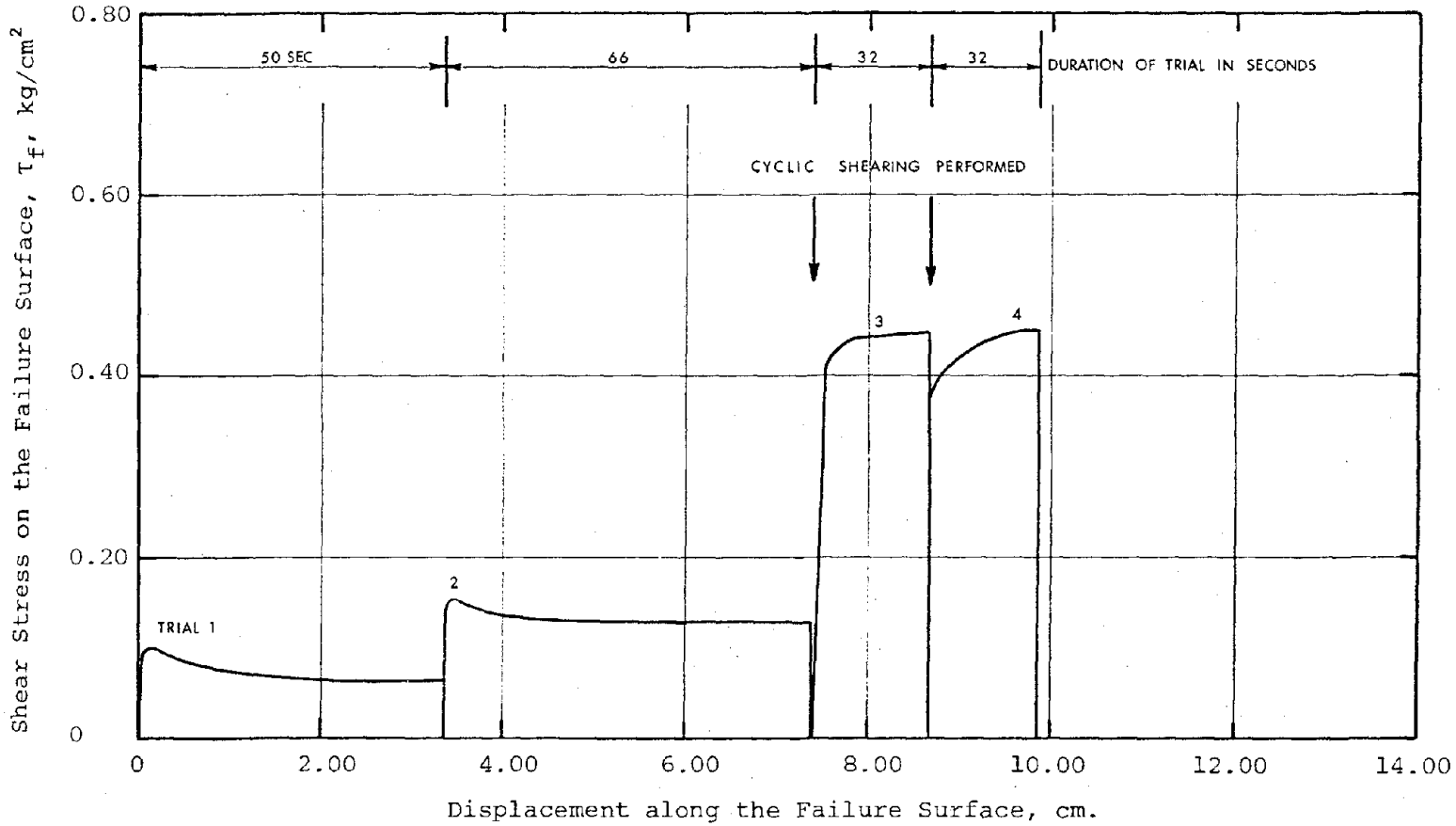

Test No. 2

Material: Banding Sand #6

State after Consolidation: $\bar{\sigma}_v = 1.00$ kg/cm^2

$e_c = 0.765$

Method of Loading: Drained Vane Shear

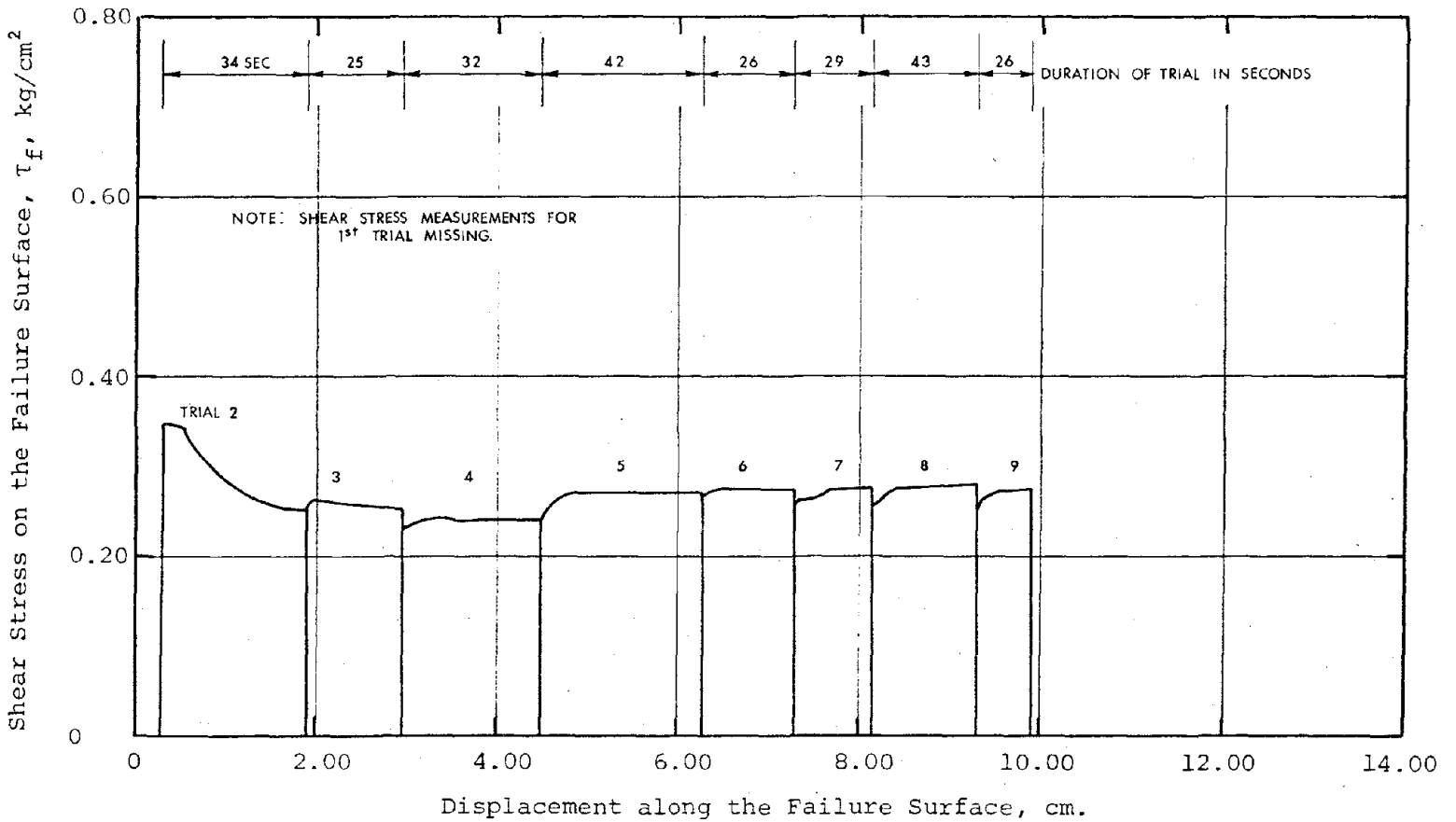

Test No. 3

Material: Banding Sand #6

State after Consolidation: $\bar{\sigma}_v = 1.00$ kg/cm^2

$e_c = 0.709$

Method of Loading: Drained Vane Shear

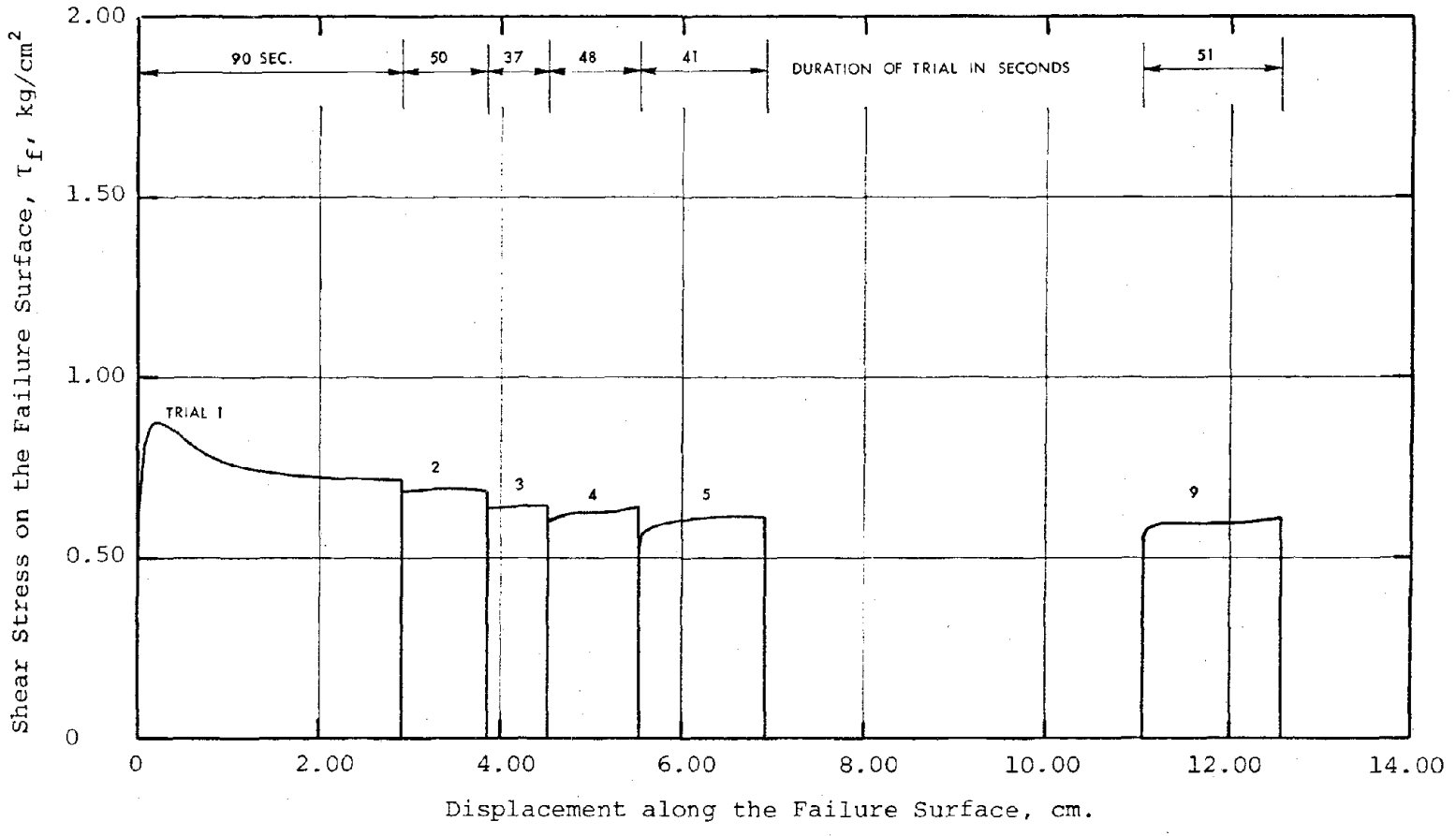

Test No. 4

Material: Banding Sand #6

State after Consolidation: $\bar{\sigma}_v = 1.00$ kg/cm^2

$e_c = 0.675$

Method of Loading: Drained Vane Shear

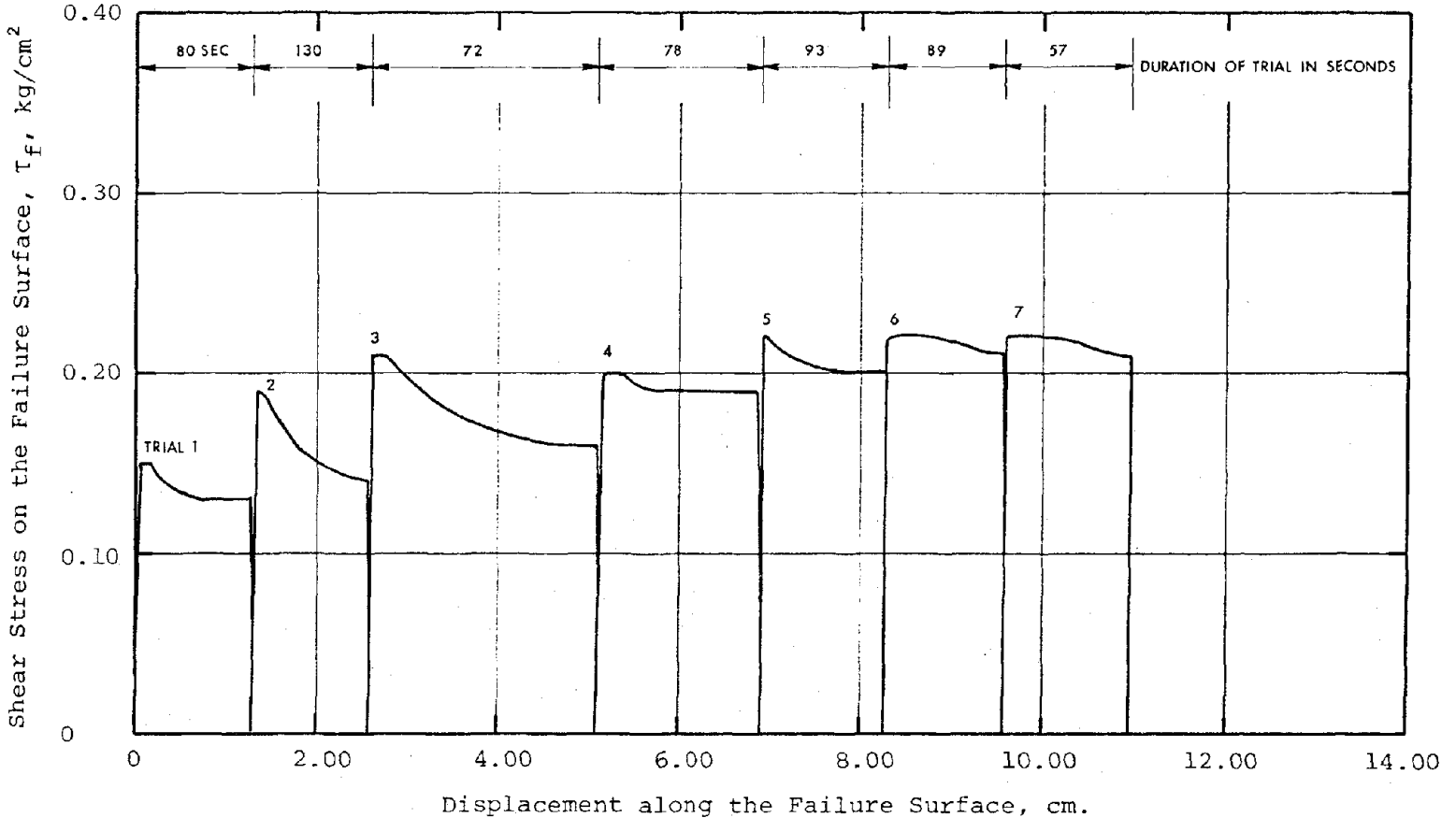

Test No. 5

Material: Banding Sand #6

State after Consolidation: $\bar{\sigma}_v$ = 1.00 kg/cm^2

e_c = 0.808

Method of Loading: Drained Vane Shear

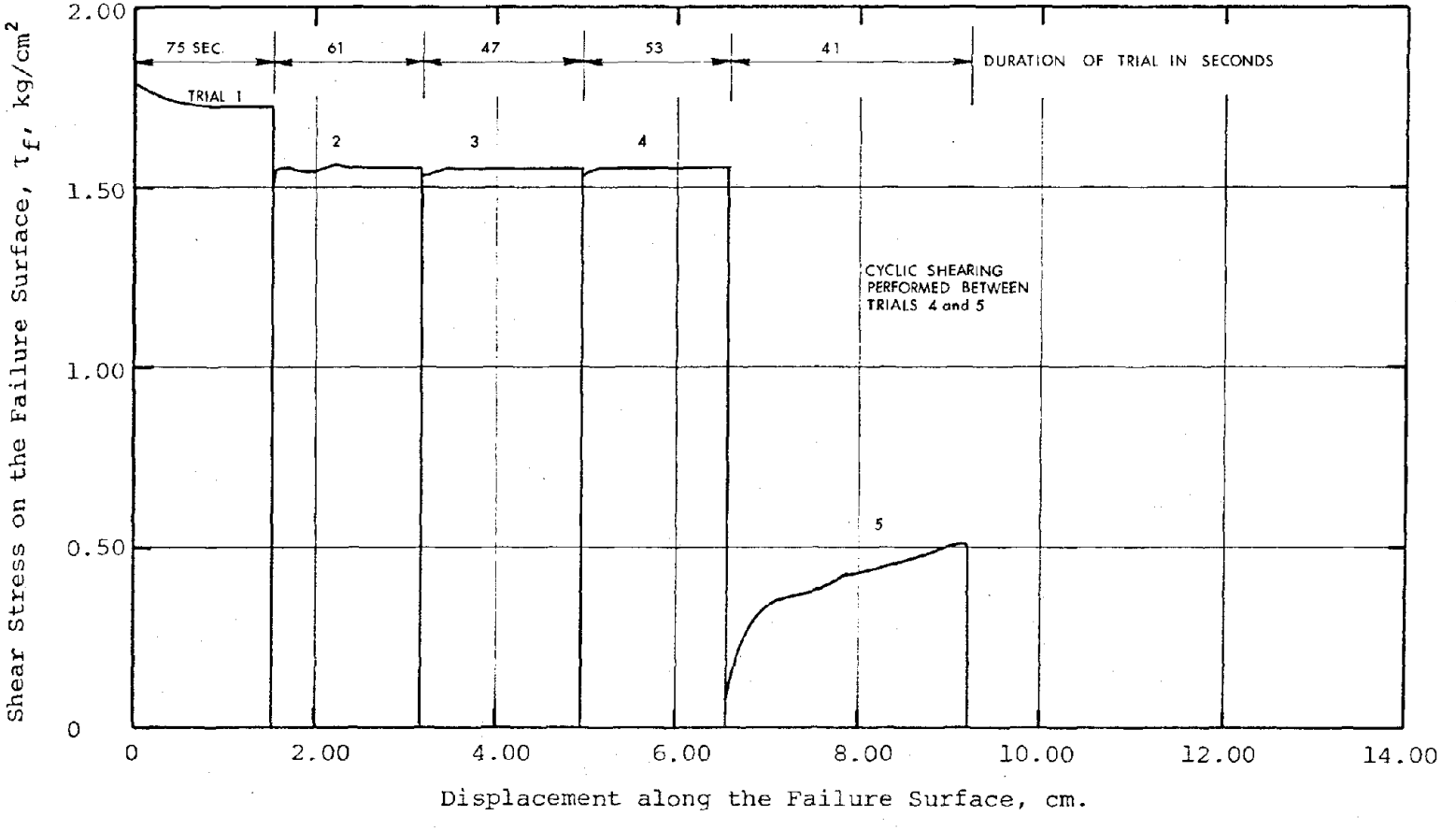

Test No. 6

Material: Banding Sand #6

State after Consolidation: $\bar{\sigma}_v = 1.00$ kg/cm^2

$e_c = 0.618$

Method of Loading: Drained Vane Shear

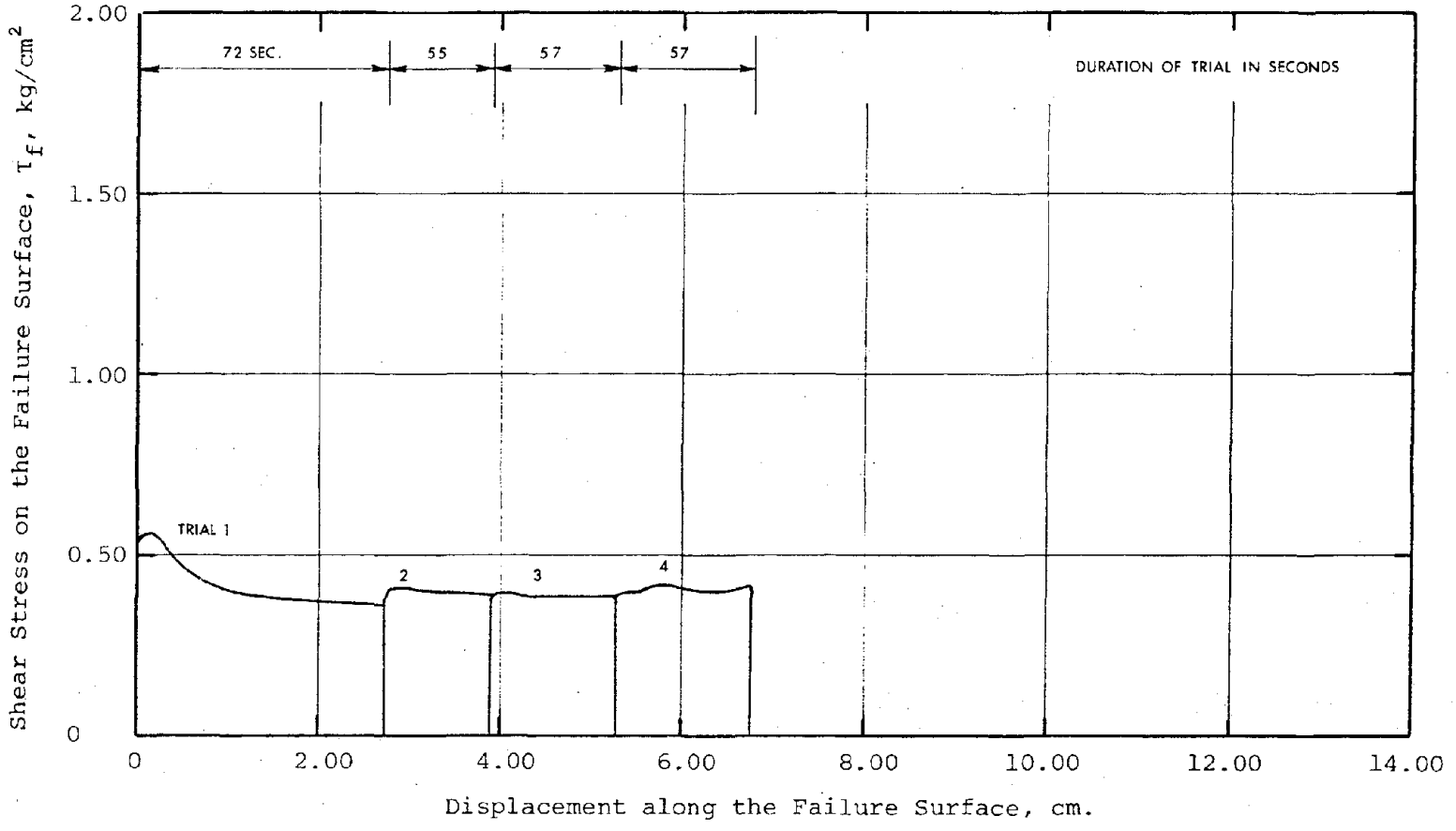

Test No. 7

Material: Banding Sand #6

State after Consolidation: $\bar{\sigma}_v$ = 1.00 kg/cm^2

e_c = 0.708

Method of Loading: Drained Vane Shear

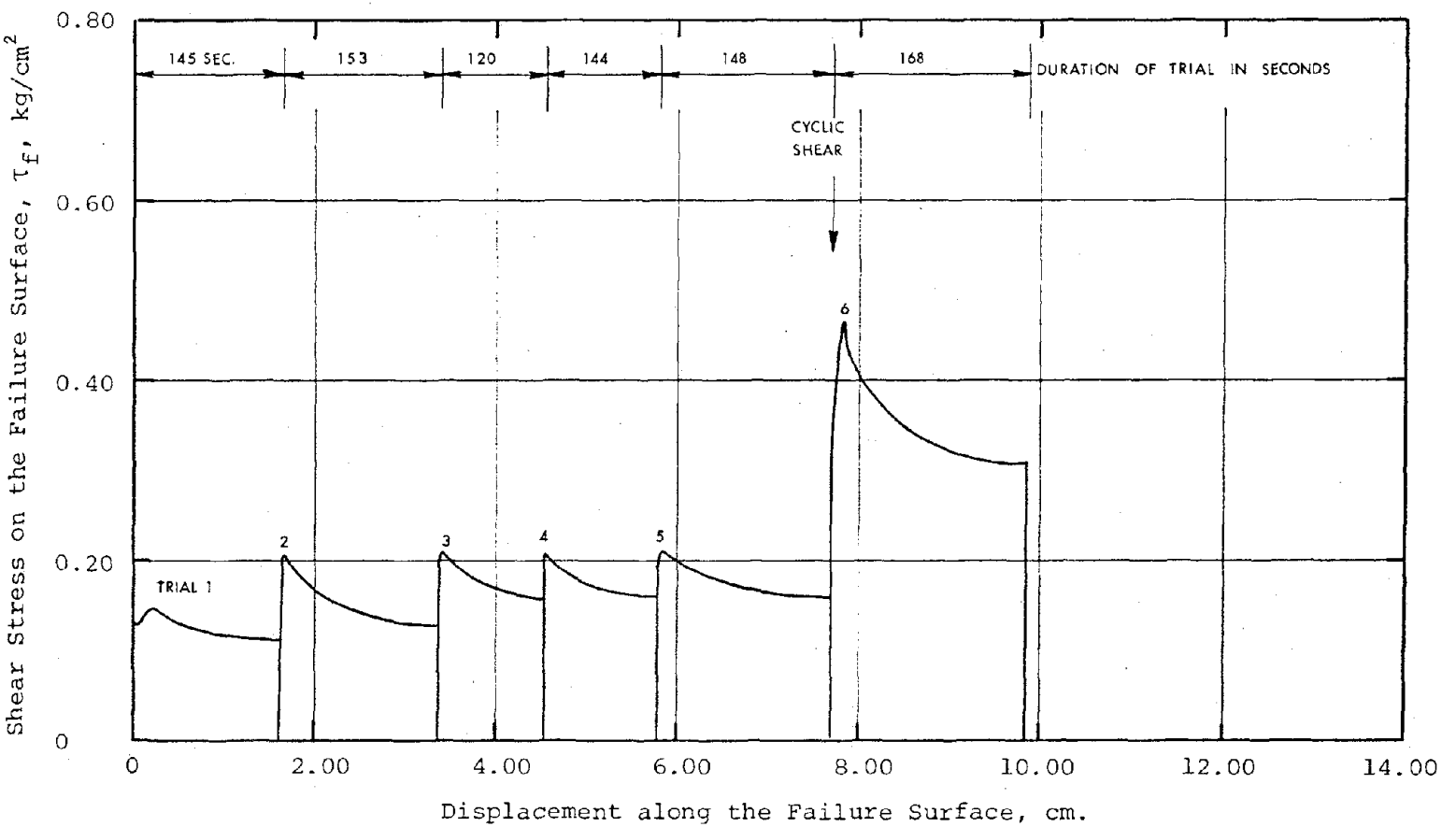

Test No. 8

Material: Mine Tailings

State after Consolidation: $\bar{\sigma}_v = 1.00$ kg/cm^2

$e_c = 1.064$

Method of Loading: Drained Vane Shear

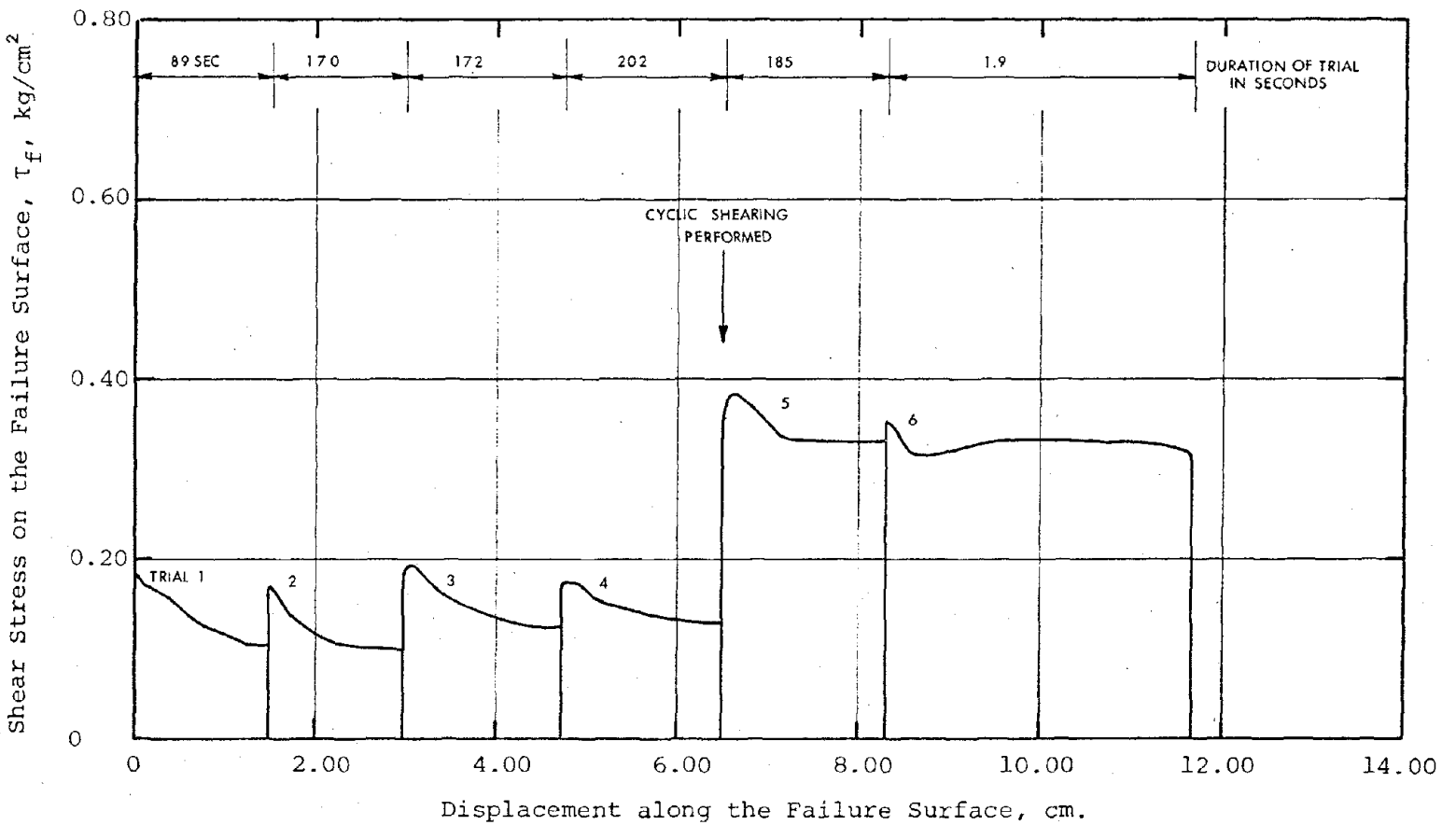

Test No. 9

Material: Mine tailings

State after Consolidation: $\bar{\sigma}_v = 1.00$ kg/cm^2

$e_c = 0.993$

Method of Loading: Drained Vane Shear

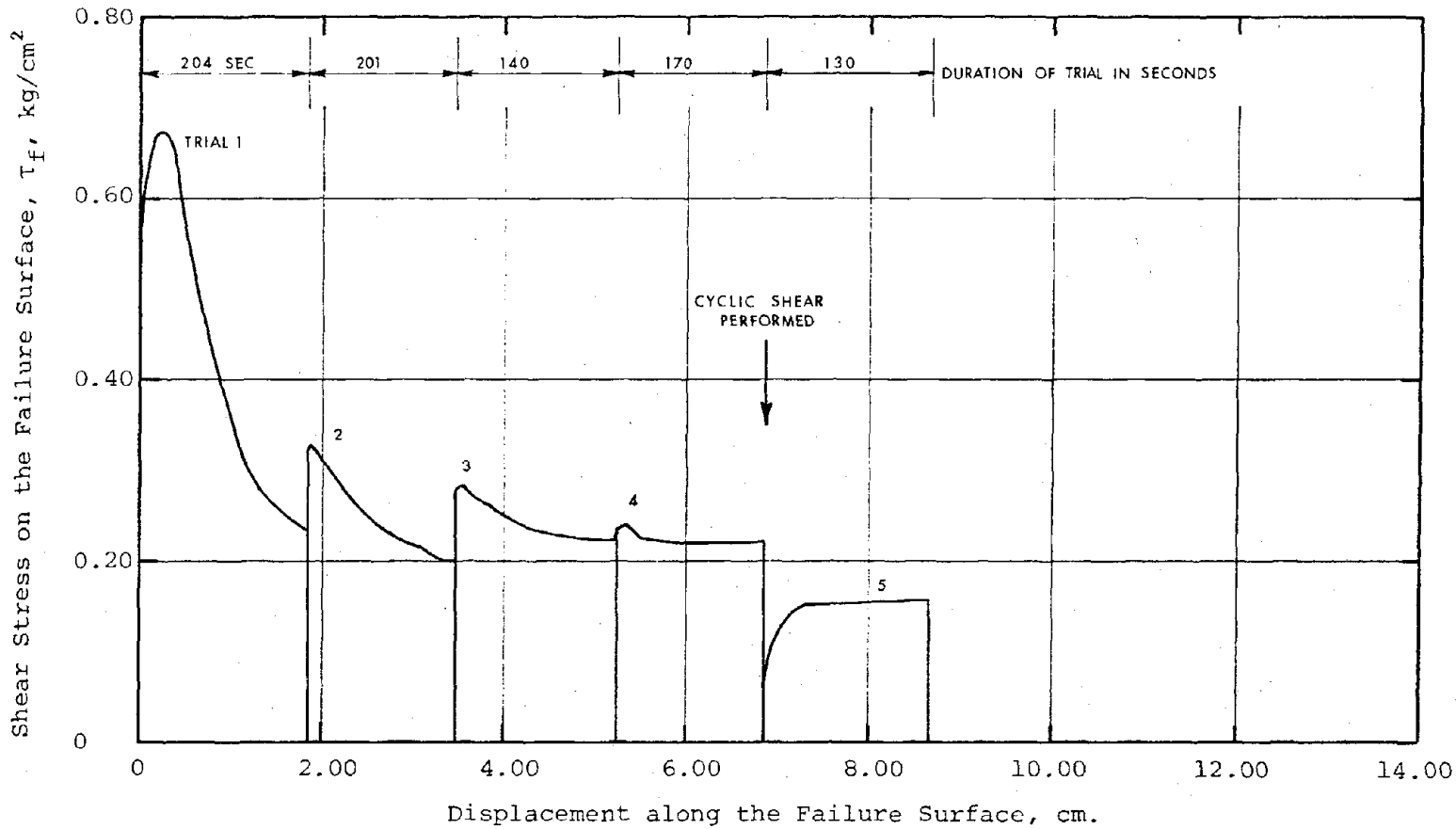

Test No. 10

Material: Mine Tailings

State after Consolidation: $\bar{\sigma}_v = 1.00$ kg/cm^2

$e_c = 0.882$

Method of Loading: Drained Vane Shear

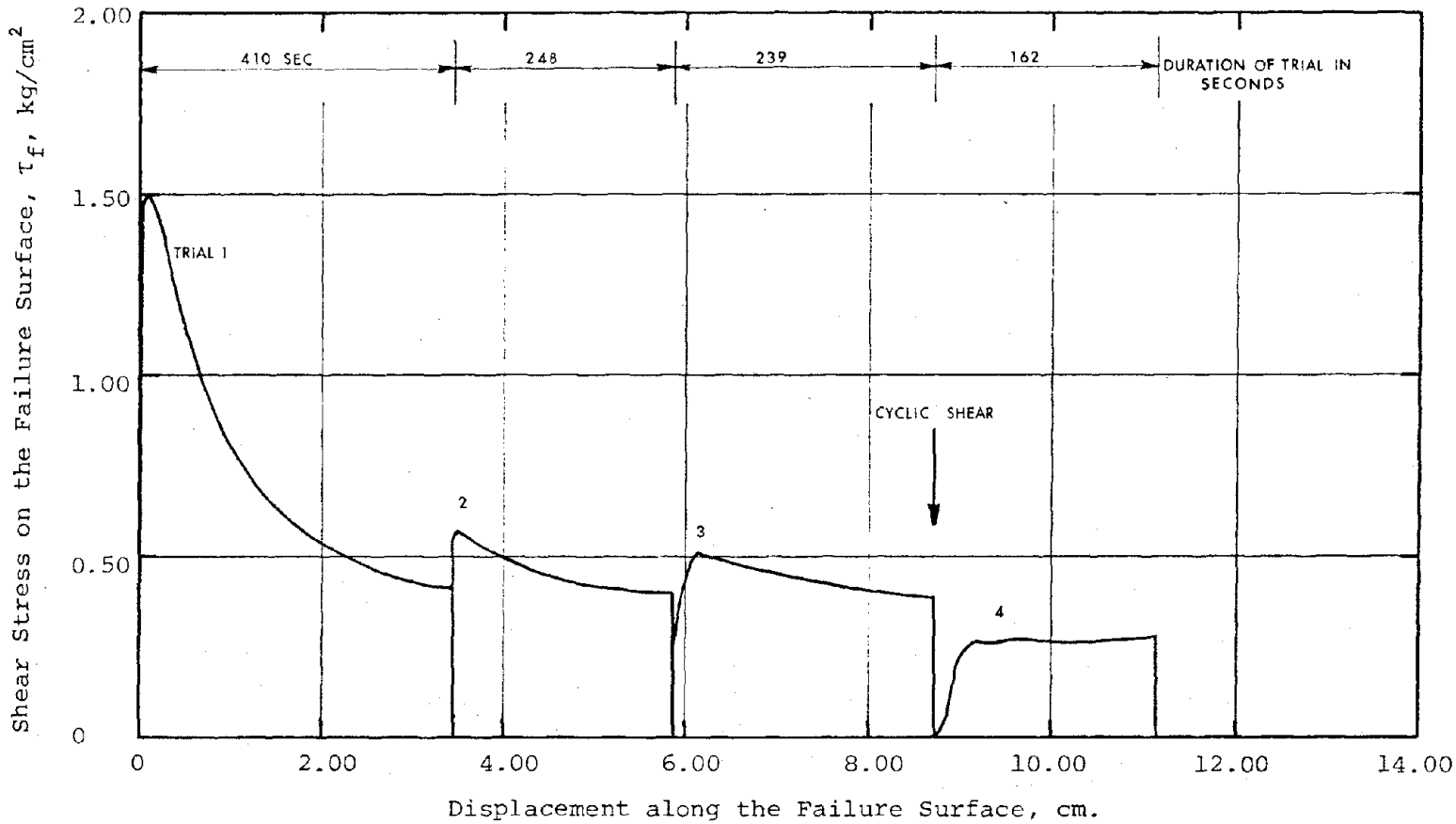

Test No. 11

Material: Mine Tailings

State after Consolidation: $\bar{\sigma}_v = 1.00$ kg/cm^2

$e_c = 0.829$

Method of Loading: Drained Vane Shear